Mathematical model of FSH-induced cAMP production in ovarian follicles

François Clement, Danielle Monniaux, John Stark, K. Hardy, J.C. Thalabard, S. Franks, D. Claude

Am J Physiol Endocrinol Metab
281: E35–E53, 2001.

Mathematical model of FSH-induced cAMP production in ovarian follicles

F. CLÉMENT,[1] D. MONNIAUX,[2] J. STARK,[4] K. HARDY,[5]
J. C. THALABARD,[3] S. FRANKS,[6] AND D. CLAUDE[1]
[1]*Institut National de Recherche en Informatique et Automatique, Unité de Recherche de Rocquencourt, Domaine de Voluceau, Rocquencourt, 78153 Le Chesnay Cedex;* [2]*Unité de Physiologie de la Reproduction et des Comportements, UMR 6073 Institut National de la Recherche Agronomique-Centre National de la Recherche Scientifique-Université F. Rabelais de Tours, 37380 Nouzilly;* [3]*Unité de Formation et de Recherche Necker, Biostatistiques-Informatique Médicale, Endocrinologie-Médecine de la Reproduction, Université Paris V, Groupe Hospitalier Necker-Enfants Malades, 75743 Paris, France;* [4]*Centre for Nonlinear Dynamics and its Applications, University College London, London WC1E 6BT;* [5]*Division of Pediatrics, Obstetrics and Gynecology, Department of Reproductive Science and Medicine, Imperial College of Science, Technology and Medicine, Hammersmith Hospital, London W12 0NN; and* [6]*Division of Pediatrics, Obstetrics and Gynecology, Department of Reproductive Science and Medicine, Imperial College of Science, Technology and Medicine, St. Mary's Hospital Medical School, London W2 1PG, United Kingdom*

Received 30 June 2000; accepted in final form 14 February 2001

Clément, F., D. Monniaux, J. Stark, K. Hardy, J. C. Thalabard, S. Franks, and D. Claude. Mathematical model of FSH-induced cAMP production in ovarian follicles. *Am J Physiol Endocrinol Metab* 281: E35–E53, 2001.—During the terminal part of their development, ovarian follicles become totally dependent on gonadotropin supply to pursue their growth and maturation. Both gonadotropins, follicle-stimulating hormone (FSH) and luteining hormone (LH), operate mainly through stimulatory G protein-coupled receptors, their signal being transduced by the activation of the enzyme adenylyl cyclase and the production of second-messenger cAMP. In this paper, we develop a mathematical model of the dynamics of the coupling between FSH receptor stimulation and cAMP synthesis. This model takes the form of a set of nonlinear, ordinary differential equations that describe the changes in the different states of FSH receptors (free, bound, phosphorylated, and internalized), coupling efficiency (activated adenylyl cyclase), and cAMP response. Classical analysis shows that, in the case of constant FSH signal input, the system converges to a unique, stable equilibrium state, whose properties are here investigated. The system also appears to be robust to nonconstant input. Particular attention is given to the influence of biologically relevant parameters on cAMP dynamics.

signal transduction; granulosa cells; follicle-stimulating hormone; cyclic adenosine monophosphate

FOLLICULOGENESIS IS THE PROCESS of growth and functional maturation undergone by ovarian follicles, from the time they leave the pool of primordial (quiescent) follicles until ovulation, at which point they release a fertilizable oocyte. Most of the developing follicles never reach the ovulatory stage but degenerate by a process known as atresia (12). The gonadotropic hormones follicle-stimulating hormone (FSH) and luteinizing hormone (LH) play a major role in the regulation of terminal follicular development through the control of proliferation and differentiation of the granulosa cells surrounding the oocyte (29). Gonadotropin secretion is, in turn, modulated by granulosa cell products such as estradiol and inhibin. During the follicular phase of the ovarian cycle, negative feedback is responsible for reducing FSH secretion, leading to the degeneration of all but those follicles selected for ovulation. Finally, positive feedback is responsible for triggering the LH ovulatory surge leading to ovulation (10). Both FSH and LH operate mainly through G protein-coupled transmembrane receptors, transducing their signal by activation of the enzyme adenylyl cyclase and production of second-messenger cyclic adenosine monophosphate (cAMP) (30).

In previous studies (6, 7), we investigated the divergent commitment of granulosa cells toward proliferation, differentiation, or apoptosis in response to their hormonal environment. Under cumulative exposure to gonadotropins, granulosa cells progressively lose their ability to proliferate and acquire a fully differentiated state. The accumulation of intracellular cAMP beyond a threshold seems to be a key point in cell cycle arrest (26), because it is believed to lead to the activation of cyclin kinase inhibitors (11). We thus believe that a better understanding of gonadotropin-induced cAMP

Address for reprint requests and other correspondence: F. Clément, Institut National de Recherche en Informatique et Automatique, Unité de Recherche de Rocquencourt, Domaine de Voluceau, Rocquencourt, BP 105, 78153 Le Chesnay Cedex, France (E-mail: Frederique.Clement@inria.fr).

The costs of publication of this article were defrayed in part by the payment of page charges. The article must therefore be hereby marked "*advertisement*" in accordance with 18 U.S.C. Section 1734 solely to indicate this fact.

production will help gain insight into changes in the rate of differentiation among granulosa cells during terminal development (8).

In CONSTRUCTION OF A SIGNAL TRANSDUCTION MODEL, we describe the mathematical model after stating the biological assumptions on which it is based; in STABILITY ANALYSIS FOR CONSTANT FSH INPUT, we focus on the analysis of the model in the case of a constant FSH level; CONTROL OF FSH-INDUCED CAMP LEVELS is devoted to the numerical application of the model; the physiological implications of these results are discussed in DISCUSSION; and mathematical details are given in APPENDIX.

CONSTRUCTION OF A SIGNAL TRANSDUCTION MODEL

Physiological Background: Transduction of the Gonadotropic Signal in Granulosa Cells

Terminal follicular development is strictly dependent on FSH supply. Before the selection of the follicle for ovulation, granulosa cells are responsive only to FSH. As follicular maturation progresses, the coupling between FSH receptor stimulation and the activation of adenylyl cyclase becomes more and more efficient, leading to a steady increase in cAMP production (13). The accumulation of FSH-induced cAMP coincides with the appearance of and subsequent dramatic increase in LH receptors, allowing LH to act as a surrogate for FSH in granulosa cells (36). Conversely, when gonadotropin, and especially FSH, plasma levels are too low to meet the follicle's trophic requirements, uncoupling of receptor stimulation with cAMP production is one of the earliest events occurring during granulosa cell death and follicular atresia (15).

The binding of FSH to its transmembrane receptors triggers an intracellular signal via the heterotrimeric G proteins. The FSH-bound receptor activates the Gα-stimulatory ($G\alpha_s$) subunit, which interacts with adenylyl cyclase to generate an increase in cyclic AMP. Once cAMP is synthesized, it either binds and activates specific protein kinases such as protein kinase A or is degraded by cyclic nucleotide phosphodiesterase (PDE) (30).

The control of cAMP levels in granulosa cells involves both fast biochemical processes, such as binding and desensitization, occurring on a time scale of a few minutes, and slower physiological processes lasting hours or even a few days, which result mainly in changing the efficiency of the enhancement of cAMP synthesis by stimulated FSH receptors via adenylyl cyclase activation. The increase in this coupling efficiency is a progressive, hormonally regulated process (29), so that the degree of maturation of a follicle can be characterized by the average cAMP level in its granulosa cells. The design of our model follows from the interactions between these contrasting biochemical and physiological dynamics. From here onward, we will focus on the dynamics of intracellular cAMP in an average granulosa cell from the time the follicle becomes able to respond to FSH in term of cAMP production.

Biological Assumptions

The model is based on the following assumptions, which are supported by the available biological knowledge on FSH signal transduction in granulosa cells during the first part of terminal follicular development.

Binding of FSH to its receptor (R_{FSH}) results in the formation of an active complex (X_{FSH})

$$\mathrm{FSH} + R_{\mathrm{FSH}} \underset{k_-}{\overset{k_+}{\rightleftharpoons}} X_{\mathrm{FSH}}$$

Bound receptors activate adenylyl cyclase (E) through a conformational change in the associated G protein

$$\mathrm{E} \overset{X_{\mathrm{FSH}}}{\curvearrowright} \mathrm{E}_{\mathrm{FSH}}$$

Activated adenylyl cyclase (E_{FSH}) synthesizes cAMP from the substrate Mg^{2+} ATP

$$\mathrm{Mg}^{2+}\mathrm{ATP} + E_{\mathrm{FSH}} \overset{\omega}{\rightarrow} \mathrm{cAMP}$$

cAMP is hydrolyzed into AMP by PDE

$$\mathrm{cAMP} \overset{k_{\mathrm{PDE}}}{\longrightarrow} \mathrm{AMP}$$

Bound receptors are subjected to a desensitization process through cAMP-mediated phosphorylation

$$X_{\mathrm{FSH}} \overset{\rho}{\rightarrow} Xp_{\mathrm{FSH}}$$

Phosphorylated inactive complexes (Xp_{FSH}) undergo internalization into the cell, where receptors are dissociated from FSH

$$Xp_{\mathrm{FSH}} \overset{k_i}{\rightarrow} R_{\mathrm{i}}$$

Internalized receptors (R_i) are recycled back to the cell membrane, whereas FSH is hydrolyzed

$$R_{\mathrm{i}} \overset{k_r}{\rightarrow} R_{\mathrm{FSH}}$$

Consideration of only those reactions relevant to follicular development allows some simplifications to be made. Reactions generating short-lived intermediary species are neglected. In particular, the cycle of G protein activation/deactivation is not modeled explicitly. The process of receptor synthesis is assumed to compensate both for intracellular receptor degradation and for the depletion of the receptor pool during cell division, so that the total number of FSH receptors in different states (free, active, phosphorylated, and internalized) remains constant (4), leading to the follow-

ing cellular cycle for FSH receptors under different states

$$\begin{array}{ccccc} \mathrm{FSH} + & R_{\mathrm{FSH}} & \rightleftharpoons & X_{\mathrm{FSH}} \\ & \uparrow & & \downarrow \\ & R_{\mathrm{i}} & \leftarrow & Xp_{\mathrm{FSH}} \end{array}$$

Finally, cAMP-independent desensitization is not taken into consideration, because its behavior during the maturation of granulosa cells is not yet known. In addition, the amount of FSH is assumed to be sufficiently large that its concentration is unaffected by binding to receptors.

Model Equations

Let R_{FSH}, X_{FSH}, Xp_{FSH}, and R_{i} be, respectively, the concentrations of free, bound active, bound inactive (phosphorylated), and internalized FSH receptors (italics indicate concentrations). Let E_{FSH} be the concentration of activated adenylyl cyclase, and let *cAMP* be the concentration of intracellular cAMP. Let k_+, k_-, k_{i}, and k_{r} be the rate constants for FSH binding, FSH unbinding, bound complex internalization, and receptor recycling to the cell membrane, respectively. The function ρ describes the (cAMP-dependent) rate of receptor desensitization. The rates of change of the concentrations are given by the following ordinary differential equations

$$\frac{\mathrm{d}R_{\mathrm{FSH}}}{\mathrm{d}t} = k_- X_{\mathrm{FSH}} + k_{\mathrm{r}} R_{\mathrm{i}} - k_+ \mathrm{FSH} R_{\mathrm{FSH}} \qquad (1)$$

$$\frac{\mathrm{d}X_{\mathrm{FSH}}}{\mathrm{d}t} = k_+ \mathrm{FSH} R_{\mathrm{FSH}} - (\rho + k_-) X_{\mathrm{FSH}} \qquad (2)$$

$$\frac{\mathrm{d}E_{\mathrm{FSH}}}{\mathrm{d}t} = \beta[\sigma X_{\mathrm{FSH}} - E_{\mathrm{FSH}}] E_{\mathrm{FSH}} \qquad (3)$$

$$\frac{\mathrm{d}cAMP}{\mathrm{d}t} = \omega E_{\mathrm{FSH}} - k_{\mathrm{PDE}} cAMP \qquad (4)$$

$$\frac{\mathrm{d}Xp_{\mathrm{FSH}}}{\mathrm{d}t} = \rho X_{\mathrm{FSH}} - k_{\mathrm{i}} Xp_{\mathrm{FSH}} \qquad (5)$$

$$\frac{\mathrm{d}R_{\mathrm{i}}}{\mathrm{d}t} = k_{\mathrm{i}} Xp_{\mathrm{FSH}} - k_{\mathrm{r}} R_{\mathrm{i}} \qquad (6)$$

Equations 1, 4, and *6* result from applying the principle of mass action. In *Eq. 4*, ATP is treated as a nonlimiting substrate at a constant concentration, and its effect is included in the kinetic constant ω. In the same way, the concentration of the enzyme PDE is included in k_{PDE}.

The desensitization rate ρ in *Eqs. 2* and *5* is a Hill function of intracellular cAMP

$$\rho(cAMP) = \frac{\alpha cAMP^{\gamma}}{\delta^{\gamma} + cAMP^{\gamma}}$$

with saturation value (α), half-saturating cAMP concentration (δ), and slope of the increase in ρ (γ) as real parameters.

This sigmoidal dependence accounts in a compact way for the phosphorylation cascade occurring downstream of cAMP, including transmembrane receptors as phosphorylation targets. Thus phosphorylation in the model is assumed to be cAMP mediated in a dose-dependent, increasing, and saturated manner. On qualitative grounds, this choice was substantiated by the critical importance of cAMP-dependent postreceptor events for desensitization (21). On quantitative grounds, the Hill function allows either for a progressive effect of cAMP level or for a rather all-or-nothing effect, depending on the value of the slope parameter γ. Besides, the phosphorylation rate is assumed to be bounded by the saturation value α, which reflects the limits in the phosphorylation capacity resulting from the balance between phosphorylation through kinases and dephosphorylation through phosphatases.

Equation 3 governs the change in the coupling variable E_{FSH} and is designed to be understood from a physiological rather than a biochemical viewpoint. β acts as a time scale parameter. Whenever it takes a low value ($\beta \ll 1$), the changes in the coupling variable E_{FSH} are slower than those of the other variables of the model. The amplification parameter σ measures the degree of signal amplification and represents the average number of adenylyl cyclase molecules activated by one bound receptor at steady state.

The choice for the right-hand term of *Eq. 3* is subject to the following physiological constraints, which make it specific to granulosa cells: *1*) there is a basal concentration of activated adenylyl cyclase ($E_0 > 0$), due to minor constitutive activity of G proteins; *2*) under cumulative exposure to FSH, the capacity for cAMP production in response to FSH stimulation increases during terminal follicular development (E_{FSH} is an increasing function as long as $\sigma X_{\mathrm{FSH}} > E_{\mathrm{FSH}}$); *3*) the increase in the efficiency of coupling is correlated with an increase in the follicle's vulnerability toward FSH supply (as soon as $\sigma X_{\mathrm{FSH}} < E_{\mathrm{FSH}}$, E_{FSH} starts decreasing); *4*) coupling and uncoupling are autoamplified processes, due to paracrine and autocrine mechanisms enhancing the follicular sensitivity to FSH (right E_{FSH} term of amplification).

Model Reduction

The total number of receptors remains constant; hence, *Eqs. 1, 2, 5,* and *6* are subject to the conservation law

$$R_{\mathrm{T}} = R_{\mathrm{FSH}} + X_{\mathrm{FSH}} + Xp_{\mathrm{FSH}} + R_{\mathrm{i}} \qquad (7)$$

where R_{T} is the constant size of the global receptor pool. We can thus replace R_{i} in *Eq. 1* by $R_{\mathrm{T}} - (R_{\mathrm{FSH}} + X_{\mathrm{FSH}} + Xp_{\mathrm{FSH}})$, reducing the system to five equations

$$\frac{\mathrm{d}R_{\mathrm{FSH}}}{\mathrm{d}t} = (k_- - k_{\mathrm{r}}) X_{\mathrm{FSH}} - (k_+ \mathrm{FSH} + k_{\mathrm{r}}) \times R_{\mathrm{FSH}} - k_{\mathrm{r}} Xp_{\mathrm{FSH}} + k_{\mathrm{r}} R_{\mathrm{T}} \qquad (8)$$

$$\frac{\mathrm{d}X_{\mathrm{FSH}}}{\mathrm{d}t} = k_+ \mathrm{FSH} R_{\mathrm{FSH}} - (\rho + k_-) X_{\mathrm{FSH}} \qquad (9)$$

$$\frac{dE_{FSH}}{dt} = \beta[\sigma X_{FSH} - E_{FSH}]E_{FSH} \quad (10)$$

$$\frac{dcAMP}{dt} = \omega E_{FSH} - k_{PDE}cAMP \quad (11)$$

$$\frac{dXp_{FSH}}{dt} = \rho X_{FSH} - k_i Xp_{FSH} \quad (12)$$

Initial values of the variables will be denoted, respectively, as R_0, X_0, E_0, $cAMP_0$, and Xp_0.

Boundedness

A basic requirement for a physiological model to be plausible is that solutions should remain bounded for all time and that concentrations should remain nonnegative. It is easy to verify (for details see APPENDIX, *Upper Bounds of Solutions*) that, as long as $k_{PDE} > 0$, this is the case in the above model for constant FSH input, so that, for any $\epsilon > 0$, there exists a $T \geq 0$, such that for all $t \geq T$

$$R_{FSH} \leq R_T, \quad X_{FSH} \leq R_T,$$
$$Xp_{FSH} \leq R_T, \quad E_{FSH} \leq \sigma R_T + \epsilon,$$
$$cAMP \leq \frac{\omega\sigma R_T}{k_{PDE}} + \epsilon$$

If $k_{PDE} = 0$, there is no mechanism for removing cAMP from the system; hence, cAMP concentrations can grow without bound. This is obviously not a physiologically realistic case.

STABILITY ANALYSIS FOR CONSTANT FSH INPUT

Quasi-Steady-State Model and Steady States

When $\beta \ll 1$, the changes in R_{FSH}, X_{FSH}, $cAMP$ and Xp_{FSH} can be considered fast compared with the change in E_{FSH}. Applying a quasi-steady-state approximation to *Eqs. 9, 11,* and *12* in case of constant FSH input leads respectively to the following relations

$$R^{\star}_{FSH} = \frac{(\rho^{\star} + k_-)}{k_+ FSH} X^{\star}_{FSH} \quad (13)$$

$$cAMP^{\star} = \frac{\omega}{k_{PDE}} E_{FSH} \quad (14)$$

$$Xp^{\star}_{FSH} = \frac{\rho^{\star}}{k_i} X^{\star}_{FSH} \quad (15)$$

Substituting this into *Eq. 8*, we obtain

$$X^{\star}_{FSH}\left[\frac{k_i k_r + \rho^{\star}(k_i + k_r)}{k_i k_r} + \frac{(\rho^{\star} + k_-)}{k_+ FSH}\right] = R_T \quad (16)$$

where

$$\rho^{\star} = \frac{\alpha\left(\frac{\omega}{k_{PDE}} E_{FSH}\right)^{\gamma}}{\delta^{\gamma} + \left(\frac{\omega}{k_{PDE}} E_{FSH}\right)^{\gamma}}$$

Hence, the quasi-steady-state assumption defines a quasi-steady-state model reducing *system 8–12* to a one-variable, nonlinear differential equation

$$\frac{dE_{FSH}}{dt} = \beta\left\{\sigma R_T / \left[\frac{k_i k_r + \rho^{\star}(k_i + k_r)}{k_i k_r} + \frac{(\rho^{\star} + k_-)}{k_+ FSH}\right] - E_{FSH}\right\}E_{FSH} \quad (17)$$

Figure 1 illustrates the degree of discrepancy, as far as the changes in E_{FSH} are concerned, between the complete and the reduced models.

Although the transient behavior of E_{FSH} is under the control of β, its steady-state E^{*}_{FSH} is not. The steady state corresponding to $E_0 > 0$ is characterized by

$$R^{*}_{FSH} = \frac{(\rho^{*} + k_-)}{k_+ FSH} X^{*}_{FSH}$$
$$E^{*}_{FSH} = \sigma X^{*}_{FSH}$$
$$cAMP^{*} = \frac{\omega\sigma}{k_{PDE}} X^{*}_{FSH} \quad (18)$$
$$Xp^{*}_{FSH} = \frac{\rho^{*}}{k_i} X^{*}_{FSH}$$

with X^{*}_{FSH} a solution of

$$X^{*}_{FSH}\left[\left(1 + \frac{k_-}{k_+ FSH}\right) + \frac{\alpha\left(\frac{\omega\sigma}{k_{PDE}} X^{*}_{FSH}\right)^{\gamma}}{\delta^{\gamma} + \left(\frac{\omega\sigma}{k_{PDE}} X^{*}_{FSH}\right)^{\gamma}} \times \left(\frac{1}{k_i} + \frac{1}{k_r} + \frac{1}{k_+ FSH}\right)\right] = R_T \quad (19)$$

By use of simple geometric reasoning, it is possible to prove that *Eq. 19* always admits a unique, positive real root (see APPENDIX, *Existence and Uniqueness of Strictly Positive Roots of Eq. 19*). This root defines the unique equilibrium state of the system. The level of intracellular cAMP at this steady state is an increasing function of the following parameters: FSH input, size of receptor pool R_T and constants k_+, k_i k_r, and δ. Conversely it is a decreasing function of k_-, k_{PDE}, and α (see proof in APPENDIX, *Control of the Steady-State Level cAMP**). The influence of the slope parameter γ is not univocal: cAMP steady-state level is either an increasing function of γ if

$$R_T < \frac{\delta k_{PDE}}{\omega\sigma}\left[\left(1 + \frac{k_-}{k_+ FSH}\right) + \frac{\alpha}{2}\left(\frac{1}{k_i} + \frac{1}{k_r} + \frac{1}{k_+ FSH}\right)\right]$$

or a decreasing one in the opposite case.

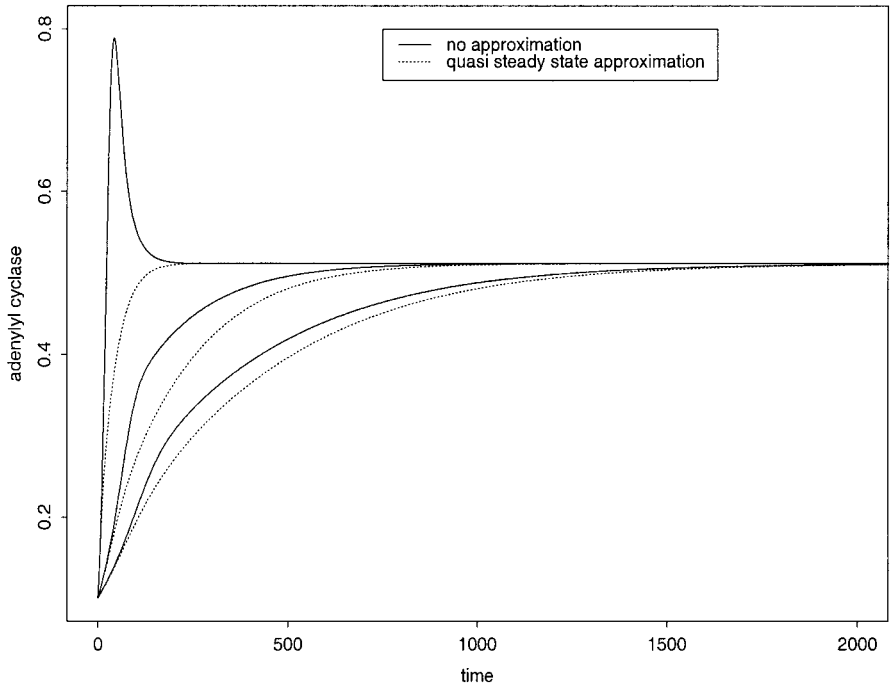

Fig. 1. Comparison between approximate and exact solution of activated adenylyl cyclase concentration (E_{FSH}). Solid lines correspond to the solutions obtained from *Eq. 10* in the complete model; dotted lines represent the solutions obtained from *Eq. 17,* assuming quasi-steady state on the other variables. From *left* to *right*, the 3 pairs of curves are respectively associated with time scale parameter (β) values of 0.1, 0.01, and 0.005. Time unit is 10^2 s, and $E_0 = 0.1 \times 10^4$ molecules/cell. Other parameter values are displayed in Table 2. The amplitude of the discrepancy between the reduced and complete models increases as β value increases, whereas the length of the transient period increases with decreasing β value.

Stability of the Steady State

Linear stability of systems of ordinary differential equations such as those arising in this paper is determined by the roots of a polynomial. The stability analysis involves the linearization of *system 8–12* in the form

$$\frac{d\mathbf{q}}{dt} = M_j\mathbf{q}$$

where $\mathbf{q}$ is the vector of the time-dependent concentrations (R_{FSH}, X_{FSH}, Xp_{FSH}, E_{FSH}, *cAMP*), and M_j is the matrix of the linearized nonlinear terms evaluated at the steady state, which is defined as the Jacobian matrix and is given by

$$M_j = \begin{bmatrix} -k_+FSH - k_r & k_- - k_r & 0 & 0 & -k_r \\ k_+FSH & -(\rho^* + k_-) & 0 & -X^*_{FSH}\partial\rho^* & 0 \\ 0 & \beta\sigma^2 X^*_{FSH} & -\beta\sigma X^*_{FSH} & 0 & 0 \\ 0 & 0 & \omega & -k_{PDE} & 0 \\ 0 & \rho^* & 0 & X^*_{FSH}\partial\rho^* & -k_i \end{bmatrix}$$

using for simplicity the notation

$$\partial\rho^* = \left(\frac{\partial\rho}{\partial cAMP}\right)_{cAMP^*} = \frac{\gamma\alpha\delta^\gamma cAMP^{*(\gamma-1)}}{[\delta^\gamma + cAMP^{*\gamma}]^2}$$

$$= \frac{\gamma\alpha\delta^\gamma + \left(\frac{\omega\sigma}{k_{PDE}}X^*_{FSH}\right)^{\gamma-1}}{\left[\delta^\gamma + \left(\frac{\omega\sigma}{k_{PDE}}X^*_{FSH}\right)^\gamma\right]^2}$$

Solutions are obtained by setting

$$\mathbf{q} = \mathbf{q}_0\, e^{\lambda t}$$

where $\mathbf{q}_0$ is the constant vector of initial values, and the eigenvalues λ are the roots of a characteristic polynomial $|M_j - \lambda I| = 0$, with I the identity matrix.

The steady state is stable if all roots λ have a negative real part. Because formal calculation did not allow us to carry through the study of the real part signs, we made use of the Hurwitz criterion (5), which derives necessary and sufficient conditions for negativity. In the case where steady-state ρ, ρ*, is saturated and can be approximated by the constant value α, the Hurwitz criterion shows that the eigenvalues of M_j have strictly negative real parts, so that the steady state is asymptotically stable (see details in APPENDIX, *Hurwitz Criterion for Linear Stability Analysis*). Application of the criterion is not so straightforward when the dependence of ρ* on *cAMP** is taken into account, so that linear stability analysis in the general case remains to be studied. However, note that, because the equilibrium in the case of a constant ρ is hyperbolic, it is locally structurally stable; hence, it will also be asymptotically stable whenever the dependence of ρ on *cAMP* is weak (16).

Controllability Analysis

Roughly speaking, a dynamic system is said to be controllable if, starting from given initial conditions, one can find an admissible control variable (here FSH) such that there exists a time for which the state variables will be steered to prescribed values. Controllability is an important feature of the model, because if the system were not controllable, the equilibrium values would be reached independently of FSH, which would be unsatisfactory for a model that we want to use for control purposes.

The study of the controllability matrix associated with the linearized system at steady state is more easily tractable (24) than that of the Jacobian matrix and allows us to conclude that the nonlinear *system 8–12* is locally strongly accessible everywhere except if $E_0 = 0$ (details in APPENDIX, *Local Control of the System*). The controllability analysis does not require the assumption of a constant FSH input, so it leads to quite general results regarding FSH input shape.

CONTROL OF FSH-INDUCED cAMP LEVELS

Dimension of Model Variables and Parameters

To handle the model equations from a numerical viewpoint, we need to know the dimensions and ranges of both variables and parameters so as to confine cAMP output values within physiological limits. As far as variables are concerned (Table 1), granulosa-specific information is available. During terminal follicular development, there are ~10^3-10^4 FSH binding sites per cell (17, 27). Experimental measurements of cAMP concentration in granulosa cells (1, 13, 19, 20) under different conditions lie in a range from 0.1 to 10 pmol/10^6 cells, roughly corresponding to 0.2 to 20 $\times$ 10^4 molecules per cell (molecular mass of cAMP is 327 Da). As far as parameters are concerned (Table 2), FSH binds its receptors with high affinity; the equilibrium dissociation constant $K_d = k_-/k_+$ is on the order of 10^{-10} M (23). The other kinetic constants are assigned ranges of values consistent with published biochemical models in other cell types (14, 32). We used physiological FSH plasma concentrations as inputs, lying in the range from 1 to 10 ng/ml, with 3 ng/ml corresponding to 10^{-10} M on the basis of an average FSH molecular mass of 3 $\times$ 10^4 Da (35). The lowest FSH values correspond to tonic secretion, whereas the highest rather correspond to the surge secretion or the level used in stimulation protocols or in vitro experiments.

Physiological Meaning of Variations in Parameter Values

Variations in the model parameter values correspond to physiological or pathological alterations in the different steps of FSH signal processing by granulosa cells. Binding equilibrium parameters (k_+, k_-) might vary among species in relation to species-specific genetic differences or even intraspecies as a result of functional mutations or receptor polymorphism affecting the extracellular domain of the FSH receptor that contains the binding site. The number of FSH receptors available for binding can be experimentally altered. For instance, the treatment of granulosa cells with neuramidase, which catalyzes the removal of cell surface sialic acid, increases specific FSH binding (25). In the model, such a treatment would result in an increase in the size of the global receptor pool (R_T). The level of adenylyl cyclase activation might differ according to genetic differences affecting the FSH receptor domain(s) responsible for G protein activation, the degree of $G\alpha_s$-intrinsic GTPase activity, or the use of adenylyl cyclase activators such as forskolin. Variations in the amplification parameter (σ) may partly account for such processes, as this parameter is related to the average number of adenylyl cyclase molecules activated by one FSH-bound receptor during its lifetime as an active form. Different values of the cAMP synthesis parameter (ω) could correspond to different types of adenylyl cyclase, as several of them have been identified (33). Signal extinction in the model is ensured by the hydrolysis of cAMP and the phosphorylation-induced desensitization of bound receptors. Variations in the hydrolysis rate (k_{PDE}) can be experimentally achieved through chronic infusion with a PDE inhibitor such as isobutylmethylxanthine (IBMX) or, conversely, through constrained overexpression of PDE in cultured cells. Similarly, infusion of kinase inhibitors such as staurosporine alters the balance between kinase and phosphatase activities and can be related to variations in the parameters of the phosphorylation rate, especially its saturation value (α). The rate of renewal of free FSH receptors results from a dynamic equilibrium between the processes of internalization, degradation, recycling, and synthesis. In the model, renewal is dependent on both the internalization ($k_{i,}$) and the recycling (k_r) rates. Finally, the time scale parameter (β) measures the speed of amplification of

Table 1. *Model variables*

Variable	Definition	Value
	Extracellular signal	
FSH	Follicle-stimulating hormone	10^{-10} M/l
	Transmembrane species	
R_{FSH}	Free FSH receptors	10^4/cell
X_{FSH}	Bound FSH receptors	10^4/cell
Xp_{FSH}	Phosphorylated FSH receptors	10^4/cell
E_{FSH}	Adenylyl cyclase	10^4/cell
	Intracellular species	
R_i	Internalized FSH receptors	10^4/cell
cAMP	Cyclic adenosine monophosphate	10^4/cell
t	*Follicular age*	10^2 s

In species, italics denote concentration.

Table 2. *Model parameters*

Parameter	Definition	Dimension	Value
k_+	FSH binding rate	/M/s	5×10^6
k_-	FSH unbinding rate	/s	3×10^{-4}
k_i	internalization rate	/s	5×10^{-4}
k_r	recycling rate	/s	5×10^{-4}
k_{PDE}	cAMP hydrolysis rate	/s	4×10^{-4}*
β	coupling parameter	dimensionless	10^{-2}†
σ	amplification parameter	dimensionless	1.0
ω	cAMP synthesis rate	/s	10^{-2}
ρ	phosphorylation rate	/s	
α	saturation value of ρ	/s	6×10^{-4}
δ	half-saturating cAMP concentration	molecules/cell	6.5×10^4‡
γ	slope of increase in ρ	dimensionless	5.0

*9×10^{-4} in Figs. 6 and 7; †0.5×10^{-2} in Fig. 9; ‡10.5×10^4 in Figs. 6 and 7.

FSH signal in granulosa cells. It integrates the role of cross talks with different signaling pathways, notably paracrine and autocrine signaling through growth factors and steroids.

For a given combination of the model parameters, variations in FSH input help to determine the range of values where the model is the most sensitive to changes in FSH levels. Besides, increasing the level of the constant FSH input illustrates how the cell is protected against an overflow in intracellular cAMP.

Control of cAMP Steady-State and Transient Levels

Study of cAMP steady-state levels. Given a fixed value of FSH input, every parameter except the time scale parameter (β) affects the value of the cAMP steady-state level *cAMP**. This value is an increasing function of FSH input, the size of receptor pool R_T, the rate constants k_+, k_i, and k_r, and the half-saturating cAMP concentration δ. Conversely it is a decreasing function of the unbinding rate k_-, the hydrolysis rate k_{PDE}, and the saturation value α. The way cAMP* is influenced by a parameter is analyzed formally in APPENDIX (*Control of the Steady-State Level cAMP**). Interestingly, the γ-parameter, which rules the rate of increase in the phosphorylation rate (the slope of the Hill function), has a nonunivocal influence on *cAMP**, depending on the value of R_T compared with a threshold value given by

$$R_{Thresh} = \frac{\delta k_{PDE}}{\omega\sigma}\left[\left(1 + \frac{k_-}{k_+ FSH}\right) + \frac{\alpha}{2}\left(\frac{1}{k_i} + \frac{1}{k_r} + \frac{1}{k_+ FSH}\right)\right]$$

For values of R_T lower than R_{Thresh}, *cAMP** is an increasing function of γ, whereas it is a decreasing function for values $>R_{Thresh}$. When $R_T = R_{Thresh}$, altering the value of γ simply has no effect. This means that, if the receptor pool is small, the cAMP steady-state level rather benefits from an almost all-or-nothing effect of cAMP level on the phosphorylation process than from a progressive, smoother effect.

Beyond this qualitative study, quantitative dose-effect-like curves can be constructed from *Eq. 19*, which amounts, in term of *cAMP**, to

$$cAMP^*\left[\left(1 + \frac{k_-}{k_+ FSH}\right) + \frac{\alpha cAMP^{*\gamma}}{\delta^\gamma + cAMP^{*\gamma}} \times \left(\frac{1}{k_i} + \frac{1}{k_r} + \frac{1}{k_+ FSH}\right)\right] = \frac{\omega\sigma R_T}{k_{PDE}}$$

These curves are displayed in Figs. 2 and 3. The range of variations for some parameters has been deliberately exaggerated beyond physiological values so as to examine a large range of cAMP steady-state-reachable levels for a given parameter.

Study of cAMP transient levels. To retrace the history of FSH-induced cAMP production, starting from a quiescent initial state, we also need to understand the transient behavior of the system before its reaching steady state. To do so, we performed a series of numerical simulations of the model using a computer program written in C language. The differential equations were integrated by means of a Runge-Kutta method of order 4 (28), with a step of 0.01 s. cAMP transient levels depend in a complicated manner on the values of the model parameters and FSH input. The same steady state can in particular be achieved in different ways depending on the value of the time scale parameter β. This parameter is the only one in the model that does not affect the steady state but instead exerts a substantial influence on the transient behavior, especially of the coupling variable E_{FSH}.

Initial values. The start of the simulation was assumed to be the point in time when FSH receptors become efficiently coupled to G proteins and start influencing intracellular cAMP production, which corresponds to the follicle's entering the FSH-responsive stage. Before this point, it is assumed that there is a minor basal level of activated adenylyl cyclase, resulting in a low basal level of cAMP production uncoupled with FSH input. Initial conditions for the differential equations *Eqs. 8–12* are set to

$$R_{FSH}(t_0) = R_T - X_0$$

$$X_{FSH}(t_0) = \frac{R_T}{k_-/(k_+ FSH) + 1}$$

$$Xp_{FSH}(t_0) = R_i(t_0) = 0$$

$$E_{FSH}(t_0) = E_0$$

$$cAMP(t_0) = cAMP_0 = \frac{\omega}{k_{PDE}} E_0$$

These correspond to the binding equilibrium between R_{FSH} and X_{FSH} and steady state for *Eq. 11* with activated cyclase level E_0 decoupled from receptor stimulation.

Influence of the receptor pool size. Figure 4 (*top*) illustrates the effects of varying the size R_T within the physiological range of $0.5–2 \times 10^4$ receptors/cell. As expected, decreasing R_T leads to a lower cAMP steady-state level. With the smallest R_T value (0.5×10^4), this cAMP level corresponds to a steady-state value of the desensitization rate ρ being much lower (0.02/s) than the saturation value α (0.06/*s*).

Influence of the binding dissociation constant. The increase in the dissociation constant, $K_d = k_-/k_+$, leads to an increase in the free receptor concentration together with a decrease in the concentration of bound receptors and its derived (phosphorylated and internalized) forms. This again affects the steady-state values *cAMP** and ρ*, with the highest value of K_d corresponding to the lowest cAMP level.

Influence of the amplification parameter. Figure 4 (*middle*) illustrates the role of the amplification parameter σ. The patterns of changes in E_{FSH} and *cAMP* are almost superimposed. The scale of the cAMP value range is dramatically increased as σ increases.

Influence of the hydrolysis parameter. A nonzero value of k_{PDE} is necessary for the cAMP concentration to reach a steady-state value. If $k_{PDE} = 0$, as can be seen on the solid line of Fig. 4 (*bottom*), signal turn-off

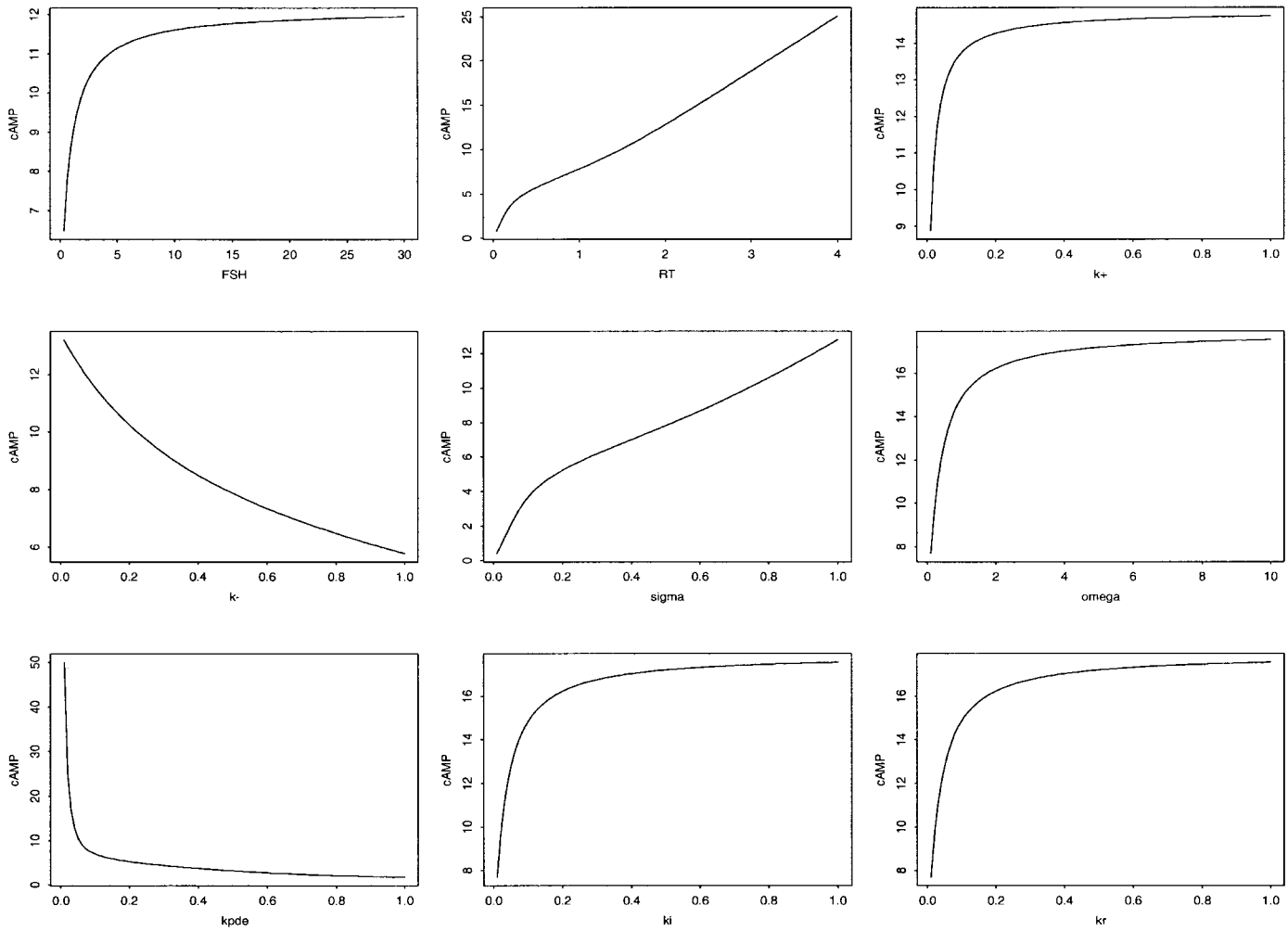

Fig. 2. Influence of follicle-stimulating hormone (FSH), size of receptor pool (R_T), FSH binding rate (k_+), FSH unbinding rate (k_-), amplification parameter (σ), cAMP synthesis rate (ω), cAMP hydrolysis rate by phosphodiesterase (k_{PDE}), phosphorylated receptor internalization rate (k_i), and internalized receptor recycling rate (k_r) on cAMP steady-state (*cAMP**) level. Panels illustrate the influence of the FSH input and other parameter values from *left* to *right* and *top* to *bottom* on *cAMP**.

is mediated only by the phosphorylation function ρ, which quickly reaches its saturation value (α) and cannot control the exponential increase in cAMP concentration. Conversely, increasing the value of k_{PDE} affects cAMP levels so as to stabilize ρ at a value far below saturation.

Influence of the phosphorylation saturation parameter. Changes in the saturation capacity of the desensitization function affect not only the steady-state level of cAMP but also the different forms of FSH receptors, as can be seen in Fig. 5. Increasing the value of α reduces the number of FSH receptors in the bound active state X_{FSH} in favor of the phosphorylated state Xp_{FSH}. The associated increase in internalized receptors cannot compensate for this imbalance even if the internalization process is at the source of free receptor renewal and hence, indirectly, of active bound receptors.

Influence of receptor renewal. Increasing either the internalization rate k_i or the recycling rate k_r allows for a quicker renewal of free FSH receptors from phosphorylated bound receptors, thus enhancing the FSH signal.

Influence of the time scale parameter. Low β values ($\beta \ll 1$) lead to a marked contrast between the dynamics of fast (R_{FSH}, X_{FSH}, *cAMP,* and Xp_{FSH}) and slow (E_{FSH}) variables, whereas high values (i.e., not much lower than 1) tend to homogenize the time scales of all the variables. As β increases from a small value toward 1, the time required to reach equilibrium is significantly decreased, as can be seen in Fig. 6. Thus, for β close to 1, the steady state is reached in a few minutes, whereas, for small values (as low as 10^{-3} in this instance), it can take several days. The maximal value reached by E_{FSH} and *cAMP* can significantly overshoot its steady-state value, and this effect also becomes more pronounced as β increases toward 1. The transient response is sensitive to even small variations in the value of β, especially for given parameter combinations. This is illustrated in Fig. 7, where the hydrolysis rate is about twice what its value is in other figures (0.09/s). The time derivative of E_{FSH} changes signs,

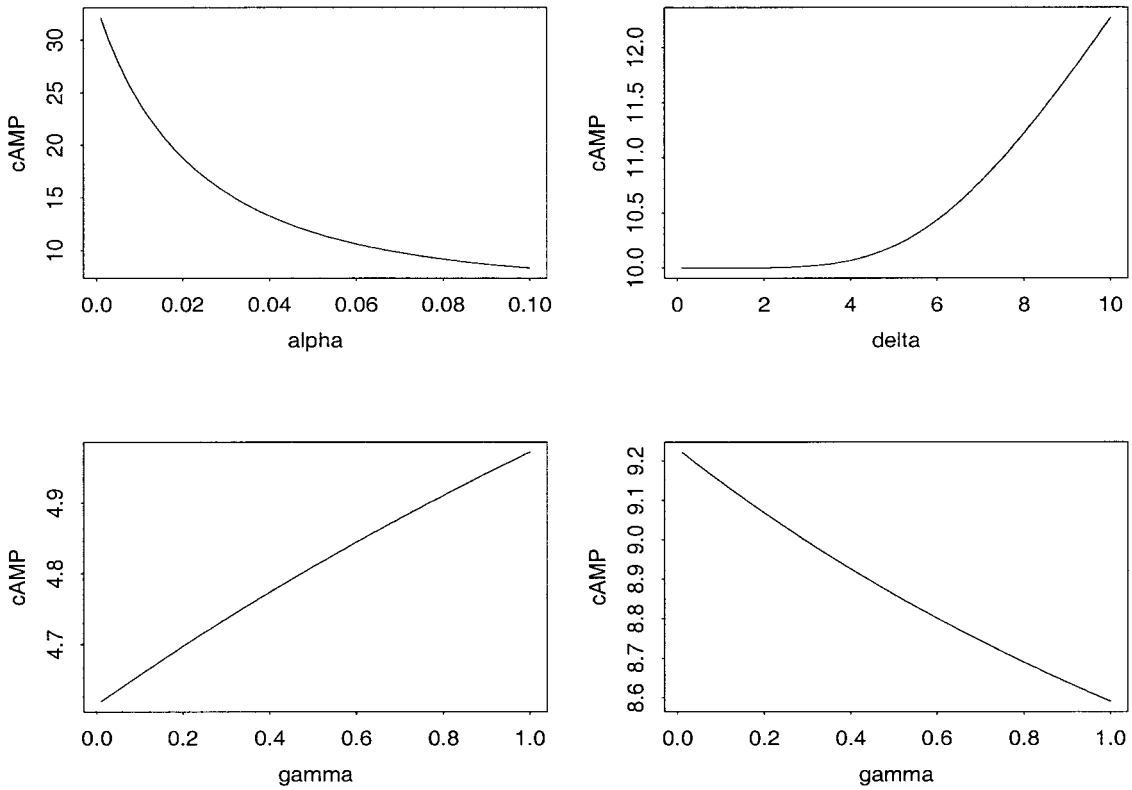

Fig. 3. Influence of saturation value of phosphorylation rate ρ (α), slope parameter (γ), and half-saturating cAMP concentration (δ) (depending on R_T value) on *cAMP**. Panels illustrate the influence of the parameters of the phosphorylation rate ρ on *cAMP**. *Top*: influence of (α) (*left*) and δ (*right*); *bottom*: influence of γ when either

$$R_T < \frac{\delta k_{PDE}}{\omega\sigma}\left[\left(1+\frac{k_-}{k_+ FSH}\right)+\frac{\alpha}{2}\left(\frac{1}{k_i}+\frac{1}{k_r}+\frac{1}{k_+ FSH}\right)\right] \quad (left)$$

or

$$R_T > \frac{\delta k_{PDE}}{\omega\sigma}\left[\left(1+\frac{k_-}{k_+ FSH}\right)+\frac{\alpha}{2}\left(\frac{1}{k_i}+\frac{1}{k_r}+\frac{1}{k_+ FSH}\right)\right] \quad (right)$$

and thus crosses its steady-state value, one or more times depending on the precise value of β, subsequently leading to a variety of *cAMP*-transient patterns.

Level and pattern of FSH input. In the physiological range from 0.3 to 3.0×10^{-10} M, a 10-fold variation in FSH concentration (Fig. 8, *top*) results in a twofold variation in cAMP level. Beyond a given level of FSH (depending on the values of the other parameters), increasing the FSH level will have almost no effect on the cAMP response. We also investigated the pattern of cAMP response to nonconstant FSH inputs (results not shown). In the case of a square-shaped FSH input, the system switches from one steady state to another as FSH switches between its high and low values. The reaction of the system to the changes in FSH input is again under the control of β. The smaller β is, the smoother the changes in the system variables, to the extent that the effects of the variation in FSH input may be perceptible only in the behavior of the receptor species (R_{FSH}, X_{FSH}, Xp_{FSH}, R_i). Other simulations with exponentially decreasing or sinusoidal FSH input yielded qualitatively similar conclusions. We show in Fig. 9 an example of the model behavior in response to real FSH data taken from Adams et al. (2; Fig. 1*B*, p. 631). The changes in FSH input are mirrored in those of free FSH receptor concentration, whereas they are quite tightly tracked by those in bound FSH receptors. The changes in phosphorylated and internalized receptors are nearly similar and follow the phosphorylation rate, which starts rising only when significant cAMP levels have been reached. The changes in activated adenylyl cyclase and cAMP are smoother. After increasing in a continuous way, they end up oscillating in a dampened manner around a steady-state value.

DISCUSSION

Our model is concerned with the cAMP dynamics resulting from FSH signal transduction in average granulosa cells of maturing ovarian follicles. We have chosen to focus on the dynamics of coupling between FSH receptor stimulation and adenylyl cyclase activation and have assumed that, on average, the cell has a constant pool of receptors. This is consistent with experimental observations that, in the first part of terminal follicular development, the increased response of cAMP production to FSH occurs in the absence of

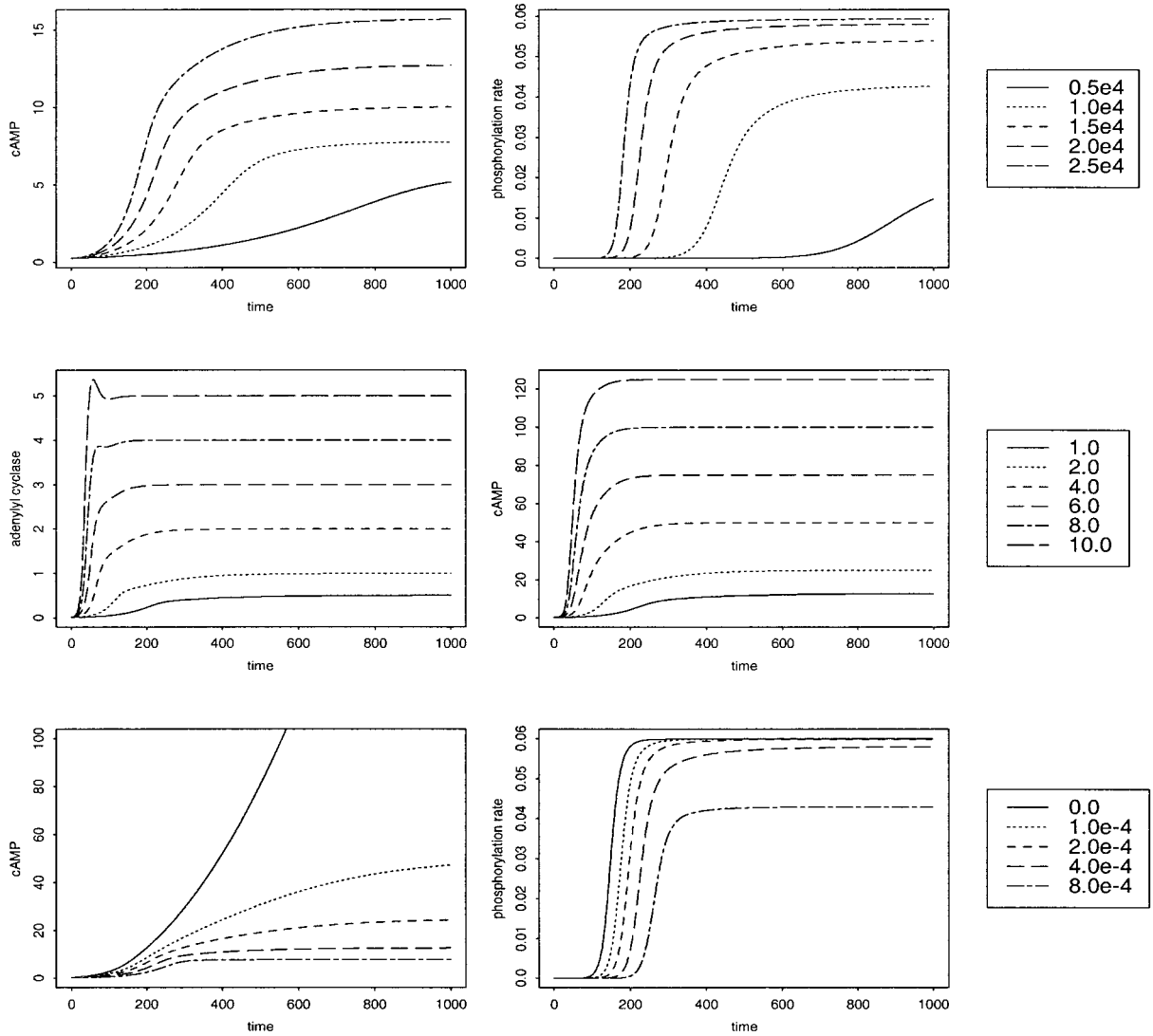

Fig. 4. Influence of R_T, σ, and k_{PDE}. *Top*: influence of R_T on changes in cAMP levels (*left*) and on changes in ρ (*right*); *inset*: nos. are in molecules/cell. *Middle*: influence of σ on changes in activated adenylyl cyclase levels (*left*) and on changes in cAMP levels (*right*); *inset*: nos. are dimensionless. *Bottom*: influence of k_{PDE} on changes in cAMP levels (*left*) and on changes in the phosphorylation rate ρ (*right*); *inset*: nos. are in k_{PDE} (/s). In this figure and in Figs. 5–9, the various panels give the time evolution of the various concentrations that constitute the variables in the model. These are expressed in units of 10^4 molecules/cell (see Table 1). The phosphorylation rate ρ is shown as a function of time. Figures 5–8, *top left,* show the pattern of applied FSH input (10^{-10} M; this is constant in Figs. 5–7). Differently styled lines on each plot of the same figure correspond to different values of the model parameter under study (displayed in *insets*), the other parameters being kept unchanged. The basic set of common parameter values is summarized in Table 2, and common initial values are $R_T = 2.0$, basal level of adenylyl cyclase (E_0) = 0.01, and $cAMP = 0.25$ (10^4 molecules/cell), with constant FSH input of 3×10^{-10} M. Time units are 10^2 s, so the simulations correspond to periods of between ~8 h and 5 days.

significant changes in the number of FSH-binding sites per granulosa cell (29). Instead, the changes in signal transduction associated with follicular development appear to affect the adenylyl cyclase enzyme system. This is corroborated by investigations on cell lines expressing the FSH receptor, in which the FSH-dependent accumulation of cAMP is highly variable but not correlated with the receptor density (reviewed in Ref. 31) and may be due to the different coupling efficiency in the different cell lines.

At the scale of a single cell, the assumption of a constant pool of receptors implies that a newborn daughter cell doubles its inherited pool of receptors (which can be considered roughly one-half of the pool of its mother cell) during the first part of G_1 after completion of mitosis. At the scale of the whole follicle, the number of receptors increases proportionally with the increase in granulosa cell number.

The notion of an average cell follows from the experimental means of investigating cAMP levels throughout follicular development. The common way of measuring cAMP is to dissect follicles and pool granulosa cells so that, even if the total number of granulosa cells increases with follicular maturation, the results are

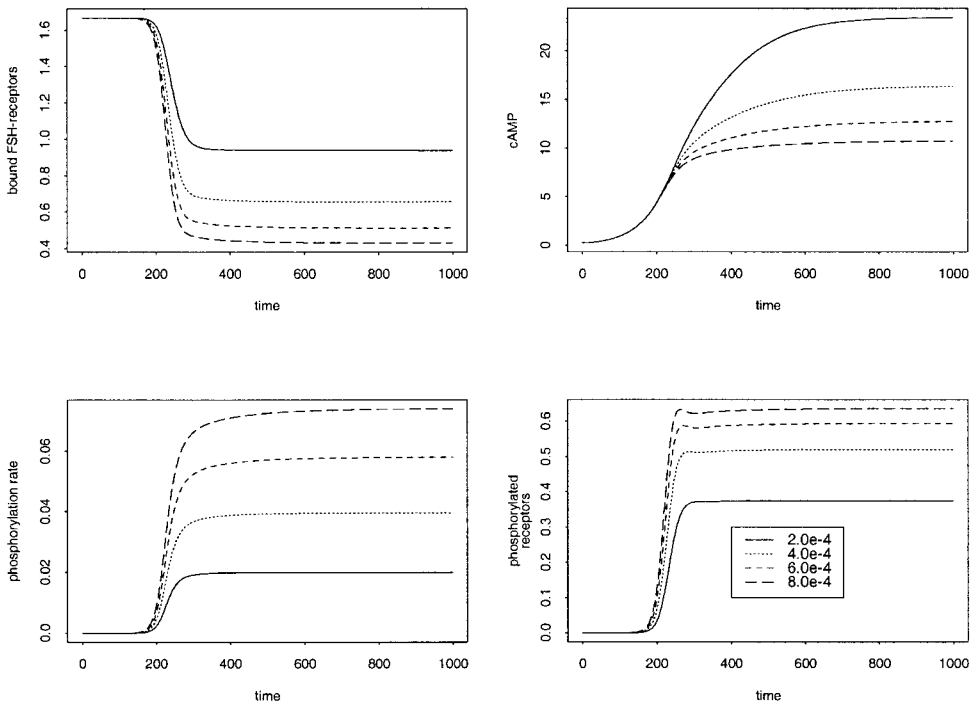

Fig. 5. Influence of the desensitization saturation capacity α (/s). *Top left*: changes in the levels of active bound FSH receptors (X_{FSH}); *top right*: changes in *cAMP* levels; *bottom left*: changes in the phosphorylation rate; *bottom right*: changes in the levels of phosphorylated bound FSH receptors (Xp_{FSH}).

expressed as average concentrations per given number of cells (usually 10^5 or 10^6) (1, 13, 19, 20). Such an average viewpoint also takes into account smoothing interactions between granulosa cells such as the exchange of cAMP molecules through gap junctions. Because the cycles of granulosa cells appear to be fully desynchronized, the average description does not need to consider the various phases of the cell cycle and moreover allows us to take into account the heterogeneous features of cell states, including the nondividing state.

To understand the nature of the most appropriate data for the model, we recall here what it really performs. The model retraces the long-term behavior of cAMP in granulosa cells during terminal follicular development in response to FSH alone. It is interested in follicles from their entering the FSH-responsive stage. For instance, in the ewe, this stage corresponds to a 1-mm diameter, compared with the 7.5-mm diameter of ovulatory follicles (monoovulating breeds). The output of the model is the cAMP level as a function of the follicle's age in response to a given pattern of FSH input. Detailed analysis has been made for constant input, but real FSH data can also be handled.

The most appropriate data would consist of repeated measurements of intracellular cAMP throughout the development of dynamically monitored follicles. Concomitantly, FSH levels should be measured. Such data could be directly exploited from the FSH-responsive to the LH-responsive stage. Once LH receptors appear on granulosa cells, cAMP production is a mixed response to both FSH and LH stimulation. To track cAMP production until the ovulatory stage, one needs to be placed in controlled situations. In physiological situations, the luteal phase in ruminant species would be the most appropriate window on the ovarian cycle to harvest data. In such species, there is no estradiol secretion from the corpus luteum, so follicular growth proceeds normally until the preovulatory size; yet LH pulsatility is low, due to high progesterone levels, so the follicles are prevented from ovulating. Hence, terminal follicular development during the luteal phase is mainly FSH dependent and thus fulfills the requirements for investigating FSH-induced cAMP production throughout terminal development. In pharmacological situations, appropriate conditions can be reproduced artificially by means of either previous desensitization with gonadotropin-releasing hormone (GnRH) agonists, or use of GnRH antagonists and administration of recombinant FSH with known bioactivity. The most limiting point in both situations is the need for dynamic, noninvasive measurements of intracellular cAMP. This might be achievable in the future through repeated ultrasound-guided follicular cell pickup as follicular development progresses. In domestic animals, follicular fluid pickup is already running well, and technical progress in devices may render direct cell pickup feasible in the medium term.

Some data on the long-term evolution of cAMP are, nevertheless, already available. The most interesting ones (13) provide information about the trends in cAMP production throughout follicular development. Unfortunately, they are not straightforward enough to handle on quantitative grounds, because cAMP concentrations are expressed against the follicular diameter. Besides, they need ovariectomy and dissection of the follicles, whose granulosa cells are pooled, so they do not allow individual or dynamic study of the follicles. cAMP levels may also be overestimated because of the use of IBMX. Despite this lack of appropriate data, we

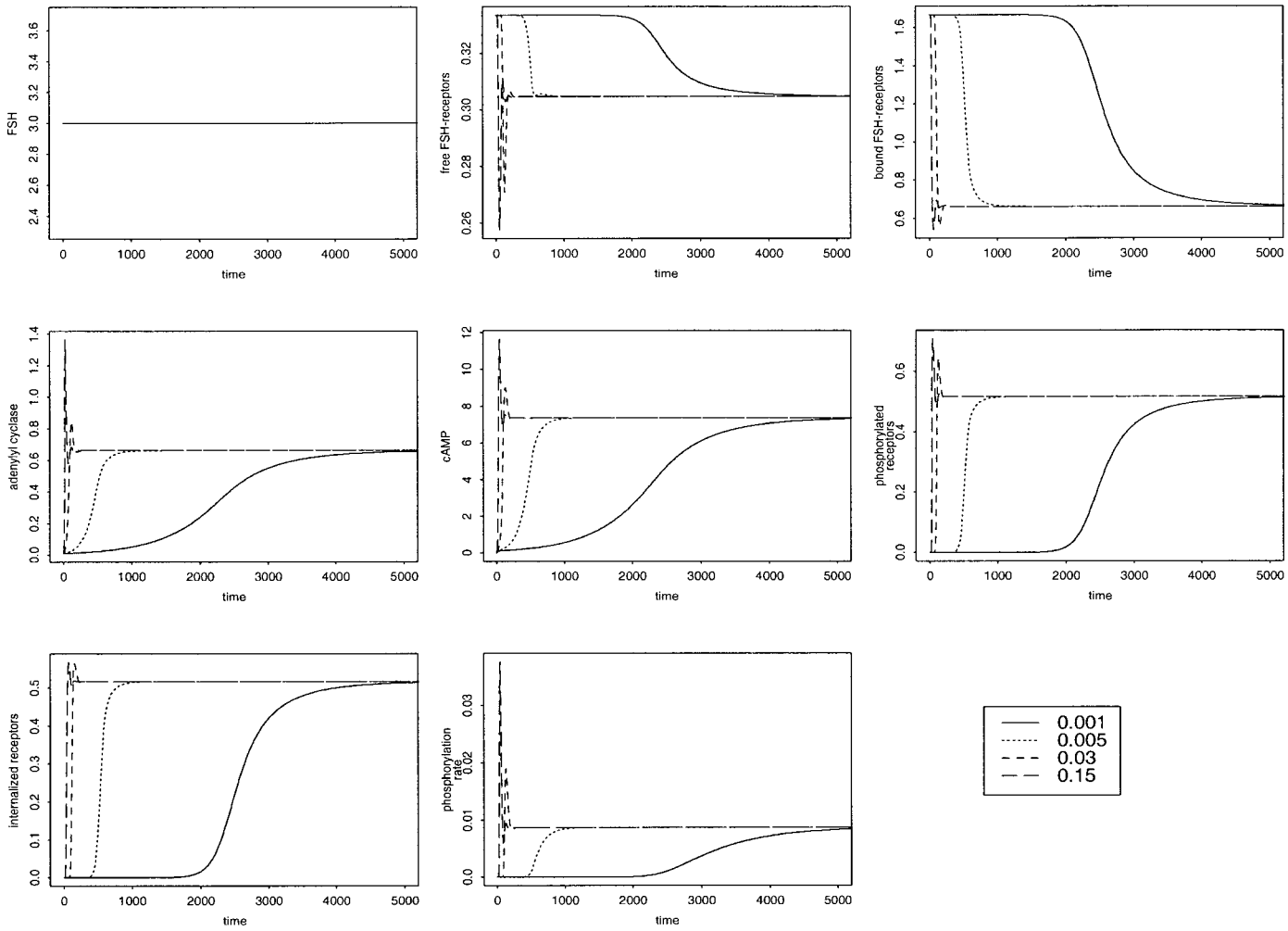

Fig. 6. Influence of the time scale parameter β (large variations), showing from *left* to *right* and from *top* to *bottom* the correspondence of each panel to the next: FSH input, changes in the levels of free FSH receptors, bound FSH receptors, activated adenylyl cyclase, cAMP, phosphorylated receptors, internalized receptors, phosphorylation rate. Inset: nos. are dimensionless.

constrained the numerical application of the model as much as we could, as is detailed in *Dimension of model variables and paramenters*.

In summary, the simulations presented in *Control of FSH-Induced cAMP Levels* have investigated the possible alterations in the capacity of the granulosa cell for FSH signal *1*) detection, *2*) relay and amplification, and *3*) overflow control. The capacity for signal detection depends on the size of the receptor pool and on the dissociation rate, which is presumably constant within a single individual but could be subject to inter- or even intraspecies differences due to the existence of gene mutations or polymorphisms. The capacity for signal relay and amplification is mediated mainly through the coupling variable E_{FSH} for activated adenylyl cyclase and the σ parameter. At this stage, our formulation of the dynamics of E_{FSH} is a "black box," subject to biological constraints. From available knowledge, one can only speculate on the underlying mechanisms. They could imply, for instance, a modulation in the intrinsic GTPase activity of different splice variants of $G\alpha_s$ subunits (9) or a shift in the balance between FSH receptor coupling with $G\alpha_s$ (activating adenylyl cyclase) and FSH receptor coupling with $G\alpha_i$ (inhibiting adenylyl cyclase). The design of new experiments would help to answer the question. They could consist, for instance, of measuring FSH-induced cAMP responses in cultured granulosa cells derived from small compared with large follicles after adding either cholera (inhibiting GTPase activity) or pertussis (inhibiting $G\alpha_i$ subunits) toxins in the culture medium. If a decrease in $G\alpha_i$ or GTPase activity occurs during terminal follicular development, one would expect to observe a greater rise in the cAMP response of treated granulosa cells, compared with control cells, from small follicles than in the response of treated cells from large follicles. The capacity for signal overflow control is exerted by means of both receptor desensitization and cAMP hydrolysis. The balance between cAMP synthesis and hydrolysis (corresponding to ω/k_{PDE}) could be related to different isoforms of adenylyl cyclase and PDE enzymes. The processes of desensitization and hydrolysis act as pro-

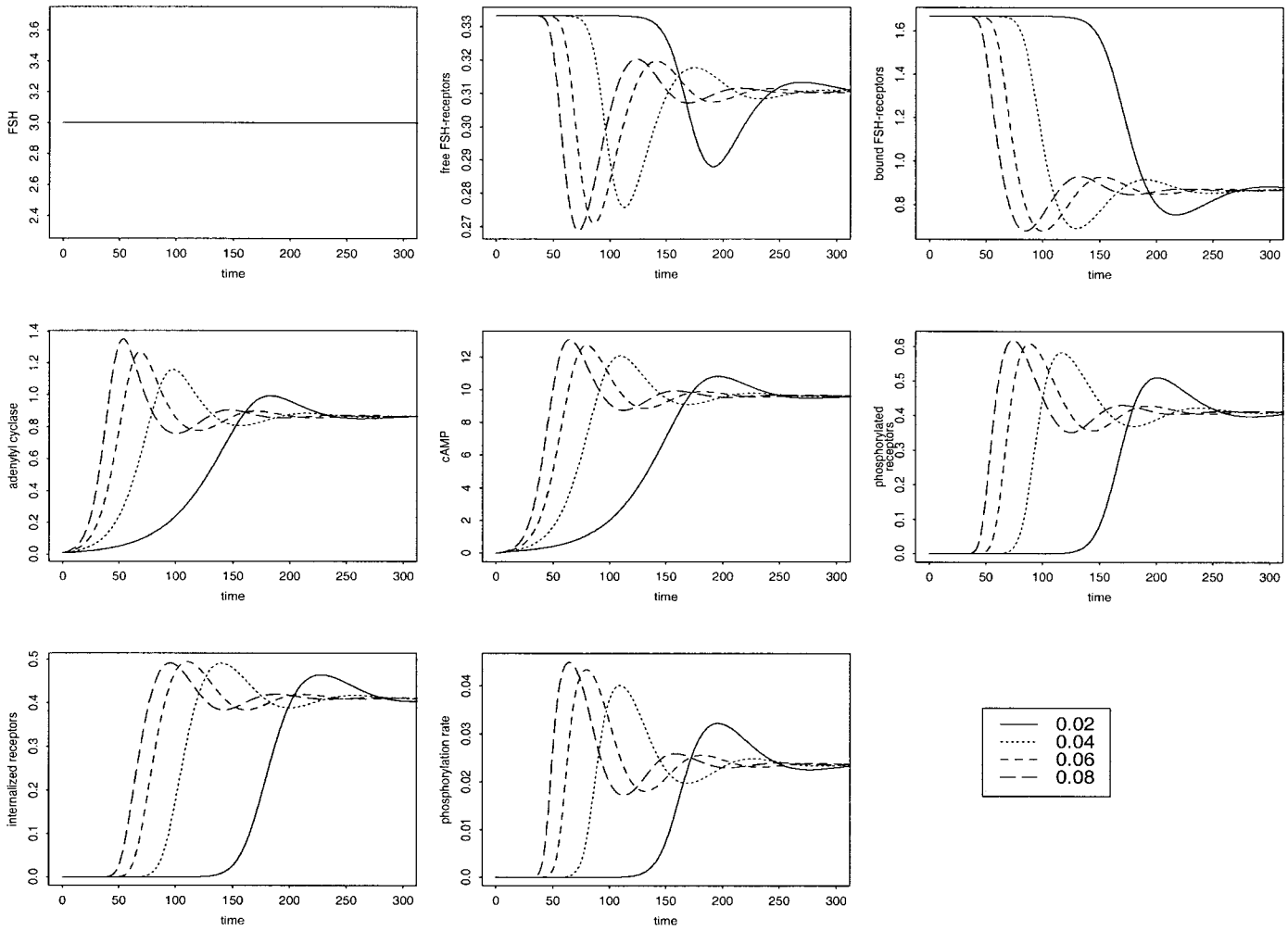

Fig. 7. Influence of β (small variations), showing from *left* to *right* and from *top* to *bottom* the correspondence of each panel to the next: FSH input, changes in the levels of free FSH receptors, bound FSH receptors, activated adenylyl cyclase, cAMP, phosphorylated receptors, internalized receptors, phosphorylation rate. *Inset*: nos. are dimensionless.

tection mechanisms of the granulosa cells against overstimulation and cAMP overflow, resulting in the control of the maximal reachable value of the intracellular cAMP level as well as of the speed in reaching a prescribed value. Early elevated levels of intracellular cAMP are known to have deleterious effects such as precocious luteinization (34). Although mathematically the system remains at this equilibrium for all time, in reality this is not the case, because the cAMP-induced expression of LH receptors around the time of selection will again modify the pattern of cAMP production. We intend to incorporate this effect in our model in the future.

The model's result that cAMP behaves as an increasing, saturating function of FSH is compatible with the observation that FSH-induced estradiol production drops for large FSH concentrations after the ovulatory surge (22). First, this drop may concern only that part of the cascade downstream of cAMP. In particular, differential regulation of protein kinase A regulatory subunits (18) could be involved, which would control the expression level of aromatase (but would not prevent LH from maintaining steroidogenesis, because it has direct, not only genic, effects such as enhancing the entry of cholesterol into the mitochondria). Second, cross talks among the various cellular signaling pathways may be of greater importance after the follicle has acquired LH receptors and affect estradiol response to FSH. Finally, the fully cAMP-dependent desensitization process of the model may be inadequate to describe what happens in the presence of large FSH concentrations. At high agonist concentration, G protein-coupled receptor kinases could also be implicated, together with the proteins of the arrestin family, in the phosphorylation of FSH receptors, as has been established for the β_2-adrenergic receptor (3).

Control of the dynamics of cAMP production in granulosa cells is a key point in the regulation of terminal follicular development. Yet, as far as we are aware, manipulation of the different steps of the cAMP cascade is not used as a way of controlling ovarian function either in domestic animals or in

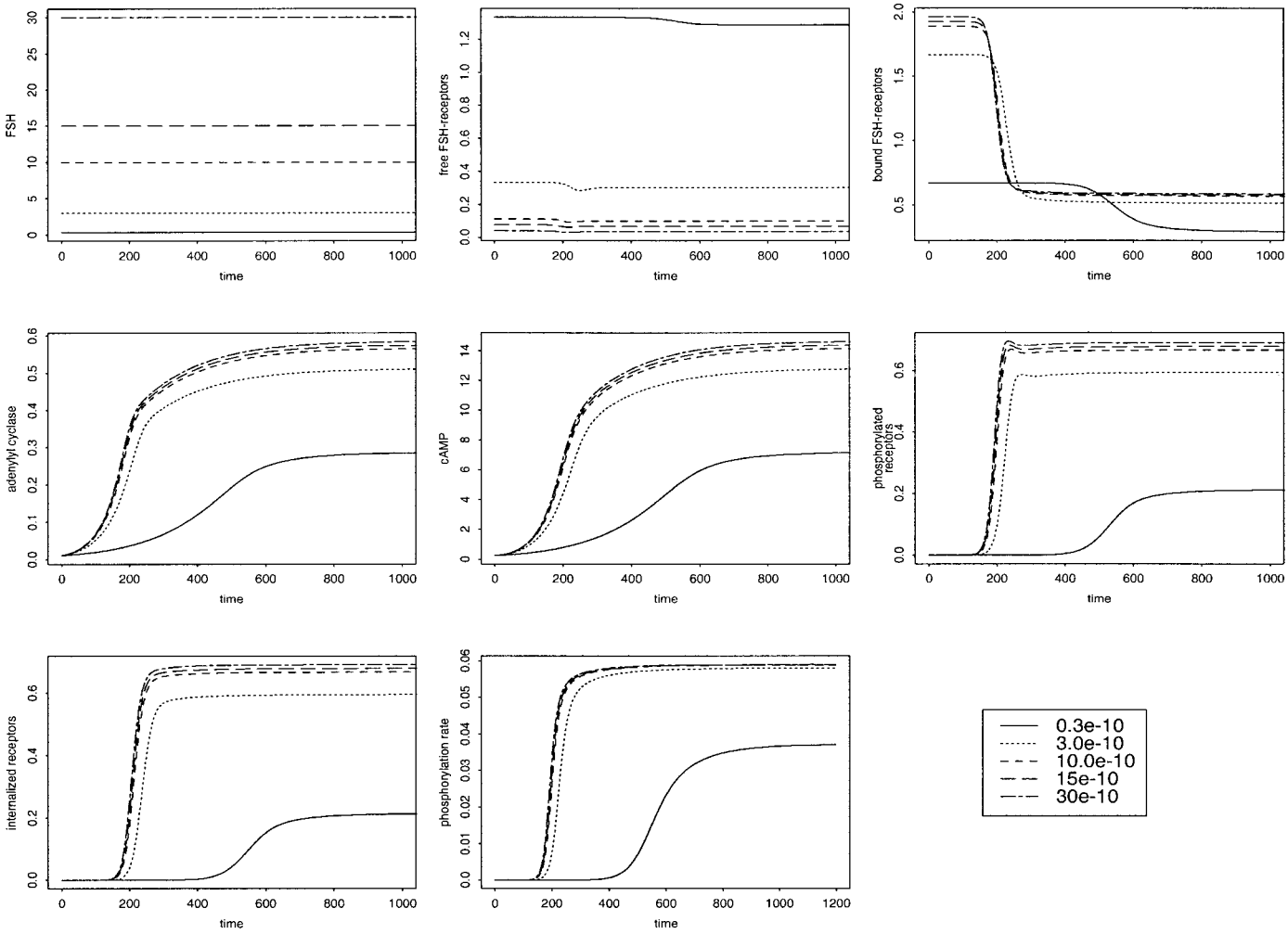

Fig. 8. Response to different levels of FSH stimulation, showing from *left* to *right* and from *top* to *bottom* the correspondence of each panel to the next: FSH input, changes in the levels of free FSH receptors, bound FSH receptors, activated adenylyl cyclase, cAMP, phosphorylated receptors, internalized receptors, phosphorylation rate. Inset: nos. are in moles per liter.

humans. A realistic model would thus be of great help in developing new strategies for the control of follicle maturation and understanding pathophysiological situations such as those encountered in polyovulating models. The Booroola Merino is a breed of sheep carrying a major gene that influences its ovulation rate. Homozygous (*F*/*F*) and heterozygous (*F*/+) carriers and noncarriers (+/+) of the gene have ovulation rates of ≥5, 3 or 4, and 1 or 2, respectively. Comparative studies (19) have shown that the *F* gene induces specific differences in follicular development because of the granulosa cells from *F*/*F* and F^+ ewes being more responsive to FSH and/or LH than granulosa cells from +/+ ewes with respect to cAMP synthesis. Similar observations have been made in polyovulating Romanov breeds compared with monoovulating Ile de France breeds (1). Furthermore, FSH-induced cAMP response was clearly greater in Romanov ewes, although the number of FSH receptors was similar, suggesting a more efficient coupling between FSH receptors and adenylyl cyclase in this breed. Interestingly, deregulation of cAMP production also seems to occur in women suffering from polycystic ovary syndrome. Premature generation of preovulatory concentrations of cAMP in granulosa cells could be at the source of anovulation (37).

The model combines biochemical and physiological angles of FSH action on granulosa cells. It helps us gain a better understanding of the dynamic control of cAMP synthesis in granulosa cells during terminal follicular development. It allows us to investigate how FSH concentrations will affect the responsiveness of follicles in terms of cAMP production. Variations in the model parameter values correspond to physiological or pathological alterations in the different steps of FSH signal processing by granulosa cells. The resulting cAMP dynamics, in turn, control the commitment of granulosa cells to proliferation, differentiation, or apoptosis. Thus understanding FSH-induced cAMP dynamics is a first step in understanding how FSH controls granulosa cell behavior on the scale of the whole follicle.

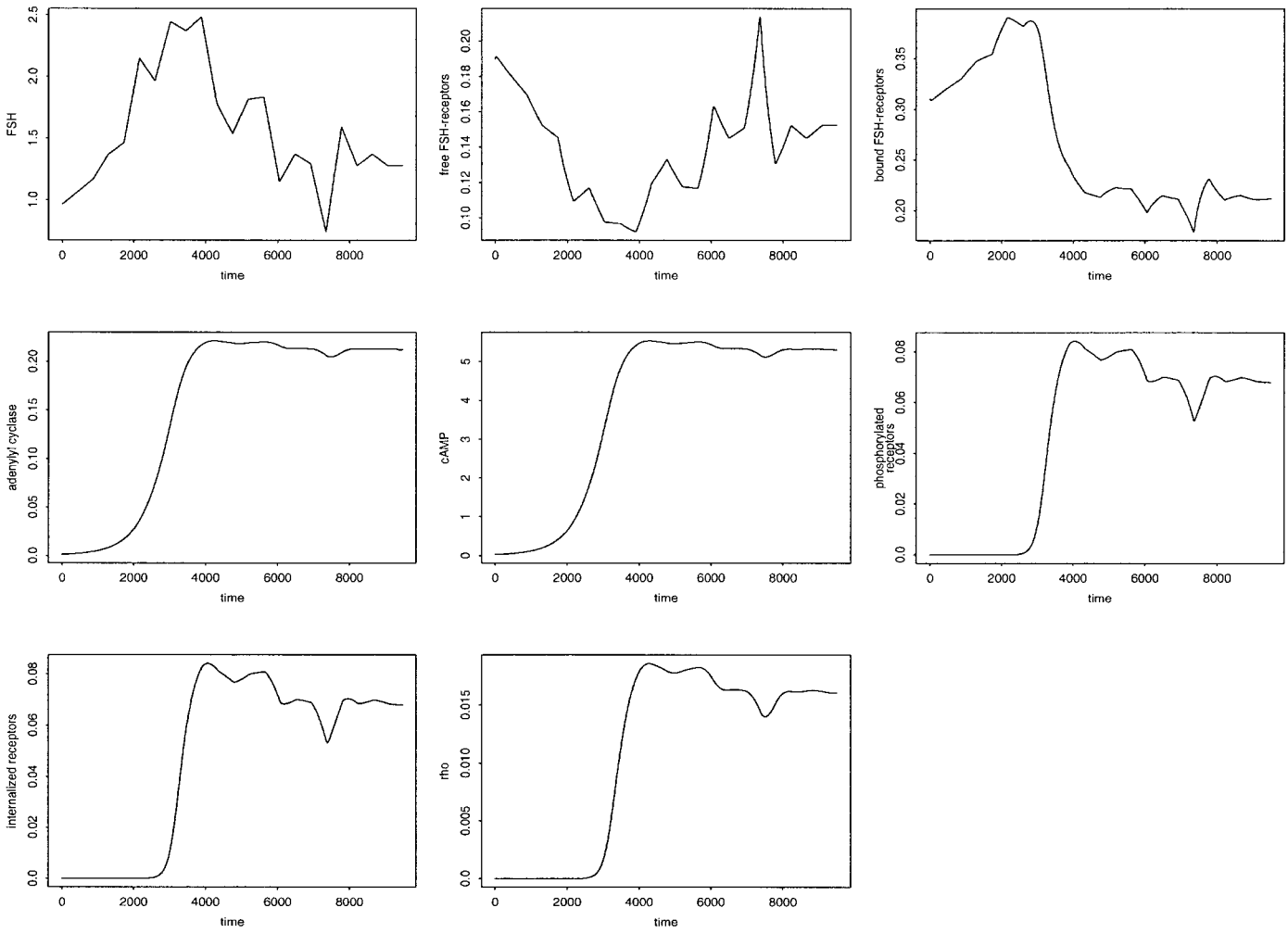

Fig. 9. Response to nonconstant FSH input (real data), showing from *left* to *right* and from *top* to *bottom* the correspondence of each panel to the next: FSH input, changes in the levels of free FSH receptors, bound FSH receptors, activated adenylyl cyclase, cAMP, phosphorylated receptors, internalized receptors, phosphorylation rate.

The main improvement to the present model would consist of giving a fully biochemically based formulation to the equation describing changes in coupling efficiency. For the moment, this remains beyond reach, because little is known about the biochemical mechanisms underlying the increase in the cAMP response of granulosa cells to FSH stimulation. Obviously, the balance between activation and inactivation of G proteins is implicated in this mechanism, but further experimental investigation is needed before a more realistic model can be built. Incorporating LH signaling is also an important challenge, because synergistic signaling by FSH and LH seems to be the basis for the selection of the ovulatory follicle(s).

Whereas inadequate response of granulosa cells to gonadotropin signals may have major repercussions on follicular development and may even lead to infertility, a realistic model characterizing both physiological and pathological signal transduction would be very useful for simulating the development of new therapeutic strategies.

APPENDIX

Upper Bounds of Solutions

From *Eqs. 1–6*, one can see that, if any one of the variables R_{FSH}, X_{FSH}, $cAMP$, Xp_{FSH}, E_{FSH}, and R_i is zero and the other variables are nonnegative, then that variable that is zero is nondecreasing. It immediately follows that, if the system starts in the physiologically relevant region with all variables nonnegative, then it remains there for all time. With the conservation equation *Eq. 7*, this implies that $R_{FSH} \leq R_T$, $X_{FSH} \leq R_T$, $Xp_{FSH} \leq R_T$, and $R_i \leq R_T$. From $X_{FSH} \leq R_T$ and *Eq. 10,* it follows that $\dot{E}_{FSH} \leq \beta(\sigma R_T - E_{FSH})E_{FSH}$. Hence, if $E_{FSH}(0) \leq \sigma R_T$, then $E_{FSH}(t) \leq \sigma R_T$ for all $t \geq 0$, whereas if $E_{FSH}(0) \geq \sigma R_T$, then, for any $\epsilon > 0$, there exists a $T \geq 0$ such that $E_{FSH}(t) \leq \sigma R_T + \epsilon$ for all $t \geq T$. Substituting this into *Eq. 11*, we see that as long as $k_{PDE} > 0$, then for any $\epsilon > 0$ there exists a $T \geq 0$ such that

$$cAMP(t) \leq \frac{\omega \sigma R_T}{k_{PDE}} + \epsilon$$

for all $t \geq T$.

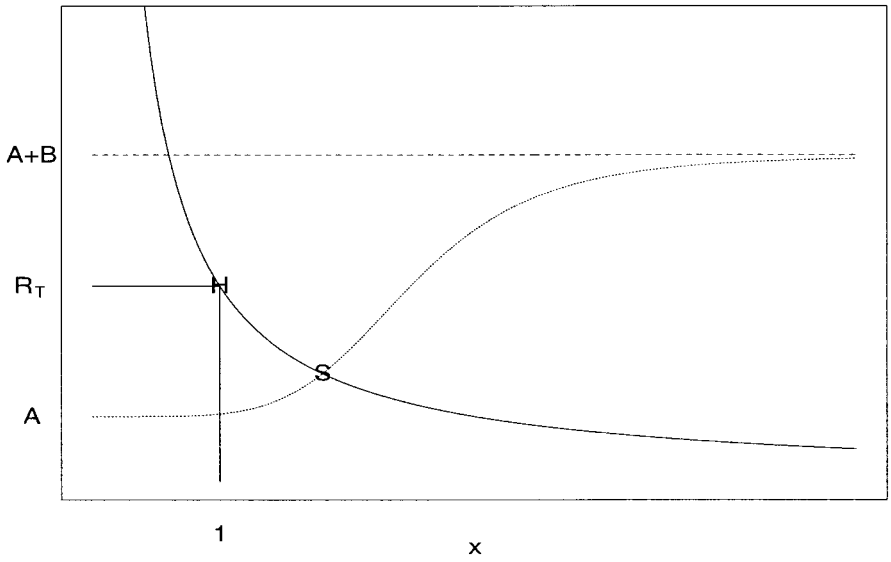

Fig. 10. Illustration of the search for the intersection point S between the hyperbola passing through point H (1, R_T) and the increasing sigmoid curve bounded by (A, A + B), which corresponds to the root of *Eq. 19*. In Figs. 10 and 11, A and B are given by

$$A = \left[1 + \frac{k_-}{k_+ \mathrm{FSH}}\right]$$

$$B = \alpha\left(\frac{1}{k_i} + \frac{1}{k_r} + \frac{1}{k_+ \mathrm{FSH}}\right)$$

Existence and Uniqueness of Strictly Positive Roots of Eq. 19

We first notice that $x = 0$ cannot be a root of *Eq. 19*. For $x > 0$, let

$$f(x) = \frac{R_T}{x}$$

and

$$g(x) = \left[\left(1 + \frac{k_-}{k_+ \mathrm{FSH}}\right) + \frac{\alpha\left(\frac{\omega\sigma}{k_{PDE}} x\right)^\gamma}{\delta^\gamma + \left(\frac{\omega\sigma}{k_{PDE}} x\right)^\gamma}\left(\frac{1}{k_i} + \frac{1}{k_r} + \frac{1}{k_+ \mathrm{FSH}}\right)\right]$$

The roots of *Eq. 19* are the points of intersection between the curves of f and g. It can be seen clearly that $f(x)$ is a strictly decreasing function of x that tends toward zero as x tends toward infinity and tends toward infinity as x tends toward zero. On the other hand, $g(x)$ is an increasing and bounded positive function of x. It follows that there can be only one intersection point for $x > 0$ and that *Eq. 19* admits one and only one strictly positive root. This geometric reasoning is illustrated in Fig. 10.

*Control of Steady-State Level cAMP**

Influence of FSH and model parameters except γ. The influence of FSH and the model parameters on *cAMP** is effected through their influence on X^*_{FSH}. Let X^{*1}_{FSH} and X^{*2}_{FSH} be the corresponding steady-state values on X_{FSH} when applying respective input FSH_1 and FSH_2, with $FSH_1 < FSH_2$. Suppose that $X^{*2}_{FSH} \le X^{*1}_{FSH}$. Because $FSH_1 < FSH_2$, we have

$$\frac{1}{k_+ \mathrm{FSH}_1} > \frac{1}{k_+ \mathrm{FSH}_2}$$

Because ρ^* is an increasing function of X^*_{FSH}

$$\frac{\alpha\left(\frac{\omega\sigma}{k_{PDE}} X^{*2}_{FSH}\right)^\gamma}{\delta^\gamma + \left(\frac{\omega\sigma}{k_{PDE}} X^{*2}_{FSH}\right)^\gamma} \le \frac{\alpha\left(\frac{\omega\sigma}{k_{PDE}} X^{*1}_{FSH}\right)^\gamma}{\delta^\gamma + \left(\frac{\omega\sigma}{k_{PDE}} X^{*1}_{FSH}\right)^\gamma}$$

Substituting into *Eq. 19* we obtain

$$R_T = X^{*1}_{FSH}\left[\left(1 + \frac{k_-}{k_+ \mathrm{FSH}_1}\right) + \frac{\alpha\left(\frac{\omega\sigma}{k_{PDE}} X^{*1}_{FSH}\right)^\gamma}{\delta^\gamma + \left(\frac{\omega\sigma}{k_{PDE}} X^{*1}_{FSH}\right)^\gamma} \times \left(\frac{1}{k_i} + \frac{1}{k_r} + \frac{1}{k_+ \mathrm{FSH}_1}\right)\right]$$

$$> X^{*2}_{FSH}\left[\left(1 + \frac{k_-}{k_+ \mathrm{FSH}_2}\right) + \frac{\alpha\left(\frac{\omega\sigma}{k_{PDE}} X^{*2}_{FSH}\right)^\gamma}{\delta^\gamma + \left(\frac{\omega\sigma}{k_{PDE}} X^{*2}_{FSH}\right)^\gamma} \times \left(\frac{1}{k_i} + \frac{1}{k_r} + \frac{1}{k_+ \mathrm{FSH}_2}\right)\right] = R_T$$

which is a contradiction. Hence, we must have $X^{*2}_{FSH} > X^{*1}_{FSH}$ whenever $FSH_1 < FSH_2$, so that

$$\frac{\partial cAMP^*}{\partial \mathrm{FSH}} > 0$$

The same reasoning applied to the parameters leads to

$$\frac{\partial cAMP^*}{\partial k_i} > 0, \frac{\partial cAMP^*}{\partial k_r} > 0, \frac{\partial cAMP^*}{\partial k_+} > 0$$

$$\frac{\partial cAMP^*}{\partial \omega} > 0, \frac{\partial cAMP^*}{\partial \sigma} > 0, \frac{\partial cAMP^*}{\partial \delta} > 0$$

and

$$\frac{\partial cAMP^*}{\partial k_-} < 0, \frac{\partial cAMP^*}{\partial k_{PDE}} < 0, \frac{\partial cAMP^*}{\partial \alpha} < 0$$

Influence of γ. Because $X^*_{FSH} > 0$, let $y = 1/X^*_{FSH}$. *Equation 19* can then be written as

$$yR_T = \left[\left(1 + \frac{k_-}{k_+ \mathrm{FSH}}\right) + \frac{\alpha}{\left(\frac{\delta k_{PDE}}{\omega\sigma} y\right)^\gamma + 1}\left(\frac{1}{k_i} + \frac{1}{k_r} + \frac{1}{k_+ \mathrm{FSH}}\right)\right]$$

Furthermore, let

$$z = \frac{\delta k_{PDE}}{\omega\sigma} y$$

then

$$\frac{\omega\sigma R_T}{\delta k_{PDE}} z = \left[\left(1 + \frac{k_-}{k_+ FSH}\right) + \frac{\alpha}{z^\gamma + 1}\left(\frac{1}{k_i} + \frac{1}{k_r} + \frac{1}{k_+ FSH}\right)\right] \quad (A1)$$

Let z_1^* and z_2^* be the roots of *Eq. A1* respectively corresponding to γ_1 and γ_2, with $\gamma_1 < \gamma_2$. Both are given through *Eq. 20* as the points of intersection of the straight line whose slope is the left-hand term in front of z, with the curve representing the right-hand term function of z. The search for this intersection point is illustrated in Fig. 11.

If

$$\frac{\omega\sigma R_T}{\delta k_{PDE}} > \left[\left(1 + \frac{k_-}{k_+ FSH}\right) + \frac{\alpha}{2}\left(\frac{1}{k_i} + \frac{1}{k_r} + \frac{1}{k_+ FSH}\right)\right]$$

both roots are <1. Hence, $z^{\gamma 1} > z^{\gamma 2}$, so that

$$\frac{\alpha}{z^{\gamma_1} + 1}\left(\frac{1}{k_i} + \frac{1}{k_r} + \frac{1}{k_+ FSH}\right) < \frac{\alpha}{z^{\gamma_2} + 1}\left(\frac{1}{k_i} + \frac{1}{k_r} + \frac{1}{k_+ FSH}\right)$$

It follows that $z^{*1} < z^{*2}$. Recalling that $z = \delta k_{PDE}/(\omega\sigma X^*_{FSH})$, we can conclude that $X^{*1}_{FSH} > X^{*2}_{FSH}$ and that

$$\frac{\partial cAMP^*}{\partial \gamma} < 0$$

On the other hand, if

$$\frac{\omega\sigma R_T}{\delta k_{PDE}} < \left[\left(1 + \frac{k_-}{k_+ FSH}\right) + \frac{\alpha}{2}\left(\frac{1}{k_i} + \frac{1}{k_r} + \frac{1}{k_+ FSH}\right)\right]$$

then

$$\frac{\partial cAMP^*}{\partial \gamma} > 0$$

Hurwitz Criterion for Linear Stability Analysis

The dependence of ρ^* on $cAMP^*$ can be neglected when the value of ρ^* is close to that of α. In this case, the $\partial\rho^*$ term vanishes, and the Jacobian matrix M_j can be rewritten as

$$M_j = \begin{bmatrix} -k_+ FSH - k_r & k_- - k_r & 0 & 0 & -k_r \\ k_+ FSH & -(\alpha + k_-) & 0 & 0 & 0 \\ 0 & \beta\sigma^2 X^*_{FSH} & -\beta\sigma X^*_{FSH} & 0 & 0 \\ 0 & 0 & \omega & -k_{PDE} & 0 \\ 0 & \alpha & 0 & 0 & -k_i \end{bmatrix}$$

The eigenvalues of M_j are given by the roots of the characteristic equation

$$\sum_{i=0}^{5} a_i \lambda^i = 0$$

We can build the following sequence of determinants associated with the a_is

$$h_1 = |a_4|, \quad h_2 = \begin{vmatrix} a_4 & a_5 \\ a_2 & a_3 \end{vmatrix}, \quad h_3 = \begin{vmatrix} a_4 & a_5 & 0 \\ a_2 & a_3 & a_4 \\ a_0 & a_1 & a_2 \end{vmatrix},$$

$$h_4 = \begin{vmatrix} a_4 & a_5 & 0 & 0 \\ a_2 & a_3 & a_4 & a_5 \\ a_0 & a_1 & a_2 & a_3 \\ 0 & 0 & a_0 & a_1 \end{vmatrix}, \quad h_5 = \begin{vmatrix} a_4 & a_5 & 0 & 0 & 0 \\ a_2 & a_3 & a_4 & a_5 & 0 \\ a_0 & a_1 & a_2 & a_3 & a_4 \\ 0 & 0 & a_0 & a_1 & a_2 \\ 0 & 0 & 0 & 0 & a_0 \end{vmatrix}$$

The signs of these determinants can be determined using a symbolic manipulation package such as Maple. This allows us to show that all of the determinants are positive, which, by the Hurwitz criterion (5), is a necessary and sufficient condition for all the eigenvalues of M_j to have strictly negative real parts. This, in turn, implies that the corresponding equilibrium is asymptotically stable.

Local Controllability of the System

In this section, we consider FSH a control variable. The linearization of *system 8–12* about the steady state can be written after separation of the state and control variables as

$$\dot{q} = M_j q + Bu \quad (A2)$$

where $q = (R_{FSH}, X_{FSH}, E_{FSH}, cAMP, Xp_{FSH})^T$, u = FSH, the Jacobian matrix M_j defines the drift vector field, and $B = (-k_+ R^*_{FSH}, k_+ R^*_{FSH}, 0, 0, 0)^T$ is the input vector field. The

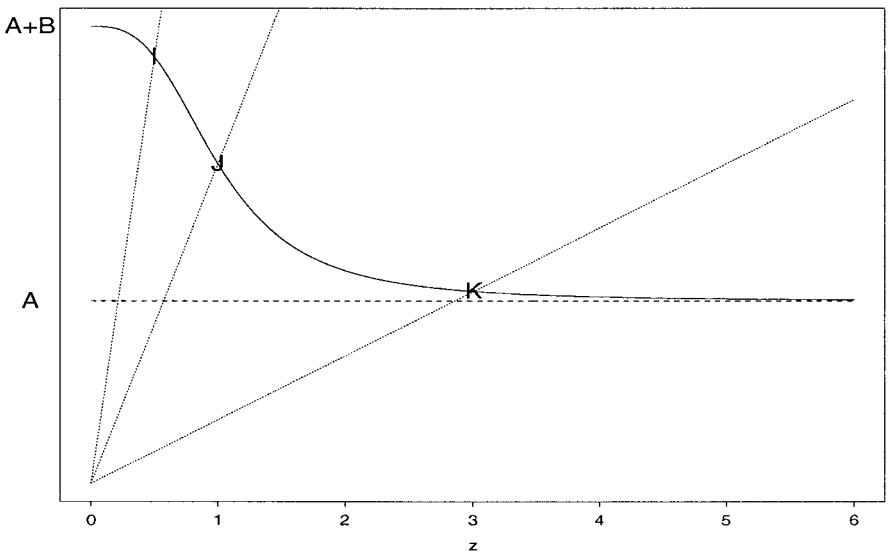

Fig. 11. Illustration of the search for the intersection point between the straight line of slope $\omega\sigma R_T/(\delta k_{PDE})$ with the decreasing sigmoid curve bounded by (A, A + B), which corresponds to the root of *Eq. 20*. The straight line passing through point J, whose coordinates are (1, A + B/2), delimits 2 distinct areas. For any intersection point whose abscissa is <1, such as I, the steady-state level of *cAMP*, $cAMP^*$, decreases as the value of γ increases. On the other hand, for any intersection point whose abscissa is >1, such as K, this level increases as the value of γ increases.

controllability matrix associated with *Eq. A2* is the square matrix whose columns are given by

$$C(M_j, B) = (B, M_jB, M_j^2B, M_j^3B, M_j^4B)$$

Formal calculation shows that the determinant of C is nonzero, which is a necessary and sufficient condition for the linearized system around the steady state to be controllable. It follows that nonlinear *system 8–12* is locally strongly accessible, which is confirmed by the study of the strong accessibility Lie algebra (24).

A similar analysis applied to the zero steady state characterized by $E_{FSH} = 0$ concludes that neither the linearized form of the system nor the nonlinear one is controllable; thus $E_{FSH} = 0$ is a strongly degenerate point for the system.

REFERENCES

1. **Abdennebi L, Monget P, Pisselet C, Remy JJ, Salesse R, and Monniaux D.** Comparative expression of luteinizing hormone and follicle-stimulating hormone receptors in ovarian follicles from high and low prolific sheep breeds. *Biol Reprod* 60: 845–854, 1999.
2. **Adams GP, Matteri RL, and Ginther OJ.** Effect of progesterone on ovarian follicles, emergence of follicular waves and circulating follicle-stimulating hormone in heifers. *J Reprod Fertil* 95: 627–640, 1992.
3. **Aittomaki K, Lucena JL, Pakarinen P, Sistonen P, Tapaneinen P, Gromoll J, Kaskikari R, Sankila EM, Lehvaslaiho H, Engel AR, Nieschlag E, Huhtaniemi I, and de la Chapelle A.** Mutation in the follicle-stimulating hormone receptor gene causes hereditary hypergonadotropic ovarian failure. *Cell* 82: 959–968, 1995.
4. **Ascoli M.** Functional consequences of the phosphorylation of the gonadotropin receptors. *Biochem Pharmacol* 52: 1647–1655, 1996.
5. **Carson RS, Findlay JK, Burger HG, and Trounson AO.** Gonadotropin receptors of the ovine ovarian follicle during follicular growth and atresia. *Biol Reprod* 21: 75–87, 1979.
6. **Cesari L.** *Asymptotic Behaviour and Stability Problems in Ordinary Differential Equations*. Berlin: Springer-Verlag, 1971.
7. **Clément F.** Optimal control of the cell dynamics in the granulosa of ovulatory follicles. *Math Biosci* 152: 123–142, 1998.
8. **Clément F, Gruet MA, Monget P, Terqui M, Jolivet E, and Monniaux D.** Growth kinetics of the granulosa cell population in ovarian follicles: an approach by mathematical modelling. *Cell Prolif* 30: 255–270, 1997.
9. **Clément F, Thalabard JC, and Claude D.** Le système de reproduction vu sous l'angle de la commande: modélisation et commande de la fonction ovarienne. In: *Modélisation et Commande de Régulations Biologiques*. Paris: Journée Thématique CNRS, 1999.
10. **DiMeglio LA and Pescovitz OH.** Disorders of puberty: inactivating and activating molecular mutations. *J Pediatr* 131: S8–S12, 1997.
11. **Europe-Finner GN, Cartwright E, Bellinger J, Mardon HJ, Barlow DH, and López Bernal A.** Identification of $G\alpha_s$ messenger ribonucleic acid splice variants in human granulosa cells. *J Mol Endocrinol* 18: 27–35, 1997.
12. **Goodman RL.** Neuroendocrine control of the ovine estrous cycle. In: *The Physiology of Reproduction*, edited by Knobil E and Neill JD. New York: Raven, 1994, p. 659–709.
13. **Graña X and Reddy EP.** Cell cycle control in mammalian cells: role of cyclins, cyclin dependent kinases (CDKs), growth suppressor gene and cyclin-dependent kinase inhibitors (CKIs). *Oncogene* 11: 211–219, 1995.
14. **Greenwald G and Roy S.** Follicular development and its control. In: *The Physiology of Reproduction*, edited by Knobil E and Neill JD. New York: Raven, p. 629–724. 1994.
15. **Henderson KM, Kieboom LE, Mac Natty KP, Lun S, and Heath D.** Gonadotrophin-stimulated cyclic AMP production by granulosa cells from Booroola × Romney ewes with and without a fecundity gene. *J Reprod Fertil* 75: 111–120, 1985.
16. **Hoffman JF, Linderman JJ, and Omann GM.** Receptor up-regulation, internalization and interconverting receptor states. Critical components of a quantitative description of N-formyl peptide-receptor dynamics in the neutrophil. *Biol Chem* 271: 18394–18404, 1996.
17. **Jolly PD, Tisdall DJ, De'ath G, Heath DA, Lun S, Hudson NL, and MacNatty KP.** Granulosa cell apoptosis, aromatase activity, cyclic adenosine 3′,5′-monophosphate response to gonadotrophins, and follicular fluid steroid levels during spontaneous and induced follicular atresia in ewes. *Biol Reprod* 56: 830–836, 1997.
18. **Katok A and Hasselblatt B.** *Introduction to the Modern Theory of Dynamical Systems.* Cambridge, UK: Cambridge Univ. Press, 1997.
19. **Knecht M, Ranta T, and Catt KJ.** Granulosa cell differentiation in vitro: induction and maintenance of follicle-stimulating hormone receptors by adenosine 3′,5′-monophosphate. *Endocrinology* 113: 949–956, 1983.
20. **Kwast-Welfeld J and Jungmann RA.** Hormonal regulation of nuclear cyclic AMP-dependent protein kinase subunit levels in rat ovaries. *J Biol Chem* 263: 14343–14350, 1988.
21. **MacNatty KP and Henderson KM.** Gonadotrophins, fecundity genes and ovarian follicular function. *J Steroid Biochem* 27: 365–373, 1987.
22. **MacNatty KP, Kieboom LE, MacDiarmid J, Heath DA, and Lun S.** Adenosine cyclic 3′,5′-monophosphate and steroid production by small ovarian follicles from Booroola ewes with and without a fecundity gene. *J Reprod Fertil* 76: 471–480, 1986.
23. **Mason HD, Mannaerts B, de Leeuw R, Willis DS, and Franks S.** Effects of recombinant human follicle-stimulating hormone on cultured human granulosa cells: comparison with urinary gonadotrophins and actions in preovulatory follicles. *Hum Reprod* 8: 1823–1827, 1993.
24. **Nakamura K, Hipkin RW, and Ascoli M.** The agonist-induced phosphorylation of the rat follitropin receptor maps to the first and third intracellular loops. *Mol Endocrinol* 12: 580–591, 1998.
25. **Nijmeijer H and van der Schatf AJ.** *Nonlinear Dynamical Control Systems.* Berlin: Springer-Verlag, 1990.
26. **Peluso JJ, Pappalardo A, and White BA.** Control of rat cell mitosis by phorbol ester-, cyclic AMP- and estradiol-17β-dependent pathways. *Biol Reprod* 49: 416–422, 1993.
27. **Perrotin F, Royere D, Roussie M, Combarnous Y, Lansac J, and Muh JP.** Characterization of human follicle-stimulating hormone binding to human granulosa cells by an immunoenzymological method. *Anal Biochem* 202: 71–75, 1992.
28. **Press WH, Flannery BP, Teukolsky SA, and Vetterling WT.** *Numerical Recipes in C, The Art of Scientific Computing*. Cambridge, UK: Cambridge Univ. Press, 1990.
29. **Richards JS.** Maturation of ovarian follicles: actions and interactions of pituitary and ovarian hormones on follicular cell differentiation. *Physiol Rev* 60: 51–89, 1980.
30. **Richards JS and Hedin L.** Molecular aspects of hormone action in ovarian follicular development, ovulation and luteinization. *Annu Rev Physiol* 50: 441–463, 1988.
31. **Simoni M, Gromoll J, and Nieschlag E.** The follicle-stimulating hormone receptor: biochemistry, molecular biology, physiology and pathophysiology. *Endocr Rev* 18: 739–773, 1997.
32. **Starbuck C and Lauffenburger DA.** Mathematical model for the effects of epidermal growth factor receptor trafficking dynamics on fibroblast proliferation responses. *Biotechnol Prog* 8: 132–143, 1992.
33. **Taussig R and Gilman AG.** Mammalian membrane-bound adenylyl cyclases. *J Biol Chem* 270: 1–4, 1995.
34. **Themmen AP, Martens JW, and Brunner HG.** Gonadotropin receptor mutations. *J Endocrinol* 153: 179–183, 1997.
35. **Ubaldi F, Camus M, Bennink HC, Van Steirteghem A, and Devroey P.** Premature luteinization in in vitro fertilization

cycles using gonadotrophin-releasing hormone agonist (GnRH-a) and recombinant follicle-stimulating hormone (FSH) and GnRH-a and urinary FSH. *Fertil Steril* 66: 275–280, 1996.

36. **Ward DN, Bousfield GR, and Moore KH.** Gonadotropins. In: *Reproduction in Domestic Animals* (4th ed.), edited by Cupps PT. London: Academic, 1991, p. 25–80.
37. **Webb R and England BG.** Identification of the ovulatory follicle in the ewe: associated changes in follicular size, thecal and granulosa cell luteinizing hormone receptors, antral fluid steroids, and circulating hormones during the preovulatory period. *Endocrinology* 110: 873–881, 1982.
38. **Willis DS, Watson H, Mason HD, Galea R, Brincat M, and Franks S.** Premature response to luteinizing hormone of granulosa cells from anovulatory women with polycystic ovary syndrome: relevance to mechanism of ovulation. *J Clin Endocrinol Metab* 83: 3984–3991, 1998.